Master's thesis

NTNU
Norwegian University of Science and Technology
Faculty of Engineering
Department of Energy and Process Engineering

Marie Karvel Kyllingstad

Energy and GHG Emission Performance Profiles at Ravneberget in Bergen – The Interplay of Onsite PV Generation, Electric Vehicles Sharing and Battery Storage for Power Peak Shaving

Master's thesis in Energy and Environmental Engineering
Supervisor: Helge Brattebø
June 2020

NTNU
Norwegian University of
Science and Technology

Marie Karvel Kyllingstad

Energy and GHG Emission Performance Profiles at Ravneberget in Bergen – The Interplay of Onsite PV Generation, Electric Vehicles Sharing and Battery Storage for Power Peak Shaving

Master's thesis in Energy and Environmental Engineering
Supervisor: Helge Brattebø
June 2020

Norwegian University of Science and Technology
Faculty of Engineering
Department of Energy and Process Engineering

NTNU

Kunnskap for en bedre verden

NTNU
Norwegian University
of Science and Technology

Department of Energy
and Process Engineering

EPT-M-2020

MASTER THESIS

for

Marie Karvel Kyllingstad

Spring 2020

Energy and GHG emission performance profiles at Ravneberget in Bergen – The interplay of onsite PV generation, electric vehicles sharing and battery storage for power peak shaving.

Ytelsesprofiler for energi og drivhusgassutslipp for Ravneberget i Bergen – Samspillet mellom solcelleproduksjon, delingsordning for elbiler og batterier for kutting av effekt-topplaster.

Background and objective

Future climate change mitigation targets will require large energy savings and GHG emission reduction in building stocks and in the mobility sector. One of the strategies as a response to these policies is the development of ZEN concepts; for instance, by urban development where the interplay of activities and subsystems at the neighbourhood level give close to zero emissions. In Norway, the ZEN Research Centre studies the energy and emission performance on a neighbourhood scale and investigates the combination of specific measures in the building/energy/mobility system and their possible benefits on the neighbourhood scale.

In 2016, Bergen municipality adopted an action plan on how the municipality should proceed to reach the 1.5 degree target. The action plan emphasizes that a collaboration between actors in the construction sector is important for increased competence and for better implementation of new smart and energy-efficient solutions in the construction projects. The Ravneberget project has been designated as an ideal pilot to test several of the solutions that contributes to sustainable development in Bergen and be at the forefront when it comes to development of ZEN concepts. With a view to develop 130 new dwellings in that area, smart solutions are needed for buildings, waste management, mobility and energy production. Investing in such solutions will also benefit the neighbourhood, reduce traffic and contribute to increased knowledge on topics such as energy efficiency and emissions reduction. A conceptual design proposal for Ravneberget, developed by Sweco, can be taken as a starting point for the neighbourhood elements.

Amongst the innovative solutions under consideration is the shared electric vehicles (EV) fleet with vehicle-to-grid (V2G) charging/discharging. The charging of these EVs may have a significant (direct or indirect) influence on the overall energy and emissions performance of the neighborhood. A detailed quantitative analysis of this influence is necessary to prevent the unfeasible design choices at the early development stages.

The overall objective of this MSc thesis is to develop a methodology that can be used in neighbourhood planning, based on a set of key performance indicators, and with Ravneberget as case study. In this work different methods are combined to analyze how a finite set of likely combinations of electric vehicles (EV) charging can interact with load profiles and photovoltaic

(PV) supply for the buildings in order to influence the energy and emission performance of the neighbourhood. It is also investigated how peak shaving and energy storage strategies affect this performance, including the interacting subsystems such as building energy demand, mobility needs, onsite energy generation, local energy storage, and import/export to external electricity grid. The emission calculations are performed by using the ZEN framework, focusing on operational emissions from energy (supply and storage), mobility solutions and embodied emissions in onsite energy generation and storage technologies.

The work is linked to IndEcol's participation in the FME-ZEN Research Centre and PhD-student Ruslan Zhuravchak's research work; hence he acts as co-supervisor. Sweco will act as a partner, contributing with inventory and guidance when feasible.

The following tasks are to be considered:

1. Carry out a literature study relevant to the work of the thesis
2. Develop a structure for the energy system at Ravneberget, including buildings, mobility, and energy supply and storage components, as a basis for an inventory of energy and emission performance analysis of the ZEN system.
3. Develop a model of the ZEN concept, applicable to the case study. Collect data and information needed to populate the model with inputs to be run, developing a set of neighbourhood charging profiles.
4. Develop a set of peak shaving strategies.
5. Discuss what are the main characteristics that influence the objective of the study, and how different core factors/variables influence the energy and environmental performance of the system. Particular attention should be given to the influence of EV charging profiles, on-site energy generation and storage, and the dynamics of emission intensity of electricity towards 2080.
6. Develop a decision support tool or methodology for neighbourhood planning containing the set of key performance indicators assessed.
7. Discuss strengths and weaknesses of your work, and suggestions for follow-up research.

-- " --

Within 14 days of receiving the written text on the master thesis, the candidate shall submit a research plan for his project to the department.

When the thesis is evaluated, emphasis is put on processing of the results, and that they are presented in tabular and/or graphic form in a clear manner, and that they are analyzed carefully.

The thesis should be formulated as a research report with summary both in English and Norwegian, conclusion, literature references, table of contents etc. During the preparation of the text, the candidate should make an effort to produce a well-structured and easily readable report. In order to ease the evaluation of the thesis, it is important that the cross-references are correct. In the making of the report, strong emphasis should be placed on both a thorough discussion of the results and an orderly presentation.

The candidate is requested to initiate and keep close contact with his/her academic supervisor(s) throughout the working period. The candidate must follow the rules and regulations of NTNU as well as passive directions given by the Department of Energy and Process Engineering.

Risk assessment of the candidate's work shall be carried out according to the department's procedures. The risk assessment must be documented and included as part of the final report. Events related to the candidate's work adversely affecting the health, safety or security, must be documented and included as part of the final report. If the documentation on risk assessment represents a large number of pages, the full version is to be submitted electronically to the supervisor and an excerpt is included in the report.

Pursuant to "Regulations concerning the supplementary provisions to the technology study program/Master of Science" at NTNU §20, the Department reserves the permission to utilize all the results and data for teaching and research purposes as well as in future publications.

The final report is to be submitted digitally in DAIM. An executive summary of the thesis including title, student's name, supervisor's name, year, department name, and NTNU's logo and name, shall be submitted to the department as a separate pdf file. Based on an agreement with the supervisor, the final report and other material and documents may be given to the supervisor in digital format.

☐ Work to be done in lab (Water power lab, Fluids engineering lab, Thermal engineering lab)
☐ Field work

Department of Energy and Process Engineering, 15. January 2020

Professor Helge Brattebø
Academic Supervisor

Research Advisor: PhD-student Ruslan Zhuravchak

Preface

This Master of Science (MSc) thesis was carried out in the spring of 2020 at the Norwegian University of Science and Technology. The work is linked to IndEcol's participation in the FME-ZEN Research Centre and the collaboration between Sweco and BKK on a zero emission neighbourhood project in Bergen. The overall objective of this MSc thesis is to contribute to the ongoing work on energy performance, generation and storage in Zero Emission Neighbourhoods (ZENs), and the related emissions occurring from implementation of different strategies and solutions.

The beginning of the semester consisted of comprehensive data collection from different sources, self-teaching of the energy simulation program *IDA ICE* and the programming language *Python*. In particular, the work related to developing an appropriate building model in IDA ICE and the programming related work, have been time consuming, and is not directly observable in the work presented. Moreover, the work in this master thesis has evolved around creating a methodology, aiming for a first draft of a scientific report to be published in collaboration with my supervisors. Throughout the semester a tight collaboration with my supervisor Helge Brattebø and co-supervisor Ruslan Zhuravchak has provided great discussions and input, generating constant progress and broader understanding of the field of ZENs. Ruslan's availability, programming skills and creativity, and Helge's excellent expertise and orientation within the research field of ZENs, have been priceless. Due to the situation of Covid-19, their support and guidance have been crucial in keeping a positive spirit and proceed with the thesis work.

The thesis consists of two parts: A scientific report, "*Energy and GHG Emission Performance Profiles at Ravneberget in Bergen – The Interplay of Onsite PV Generation, Electric Vehicles Sharing and Battery Storage for Power Peak Shaving.*", and a Supplementary material. The Supplementary material provides a broader and more transparent understanding of the background assumptions and calculations conducted in the paper. Codes can be provided if needed.

I would like to thank my head supervisor Helge Brattebø for valuable guidance and feedback during the work with this master thesis. I would also like to thank Ruslan Zhuravchak for close follow-up, discussions and support during the work on this thesis. To my contact person in Sweco, Ørjan Kongsvik Aall, I am grateful for the great trust and support, and I would also like thank Øystein Lunde in Sweco for valuable contribution on the building energy model. Lastly, I would like to thank friends and family for their endless love and support during my time as a student on NTNU, and especially during the past few months with the unusual circumstances due to Covid-19.

Abstract

Future climate change mitigation targets will require large energy savings and GHG emission reduction in the building stock and mobility sector, and the development of zero emission neighbourhood concepts are a response to these mitigation strategies. In this study we develop a methodology that can be used in neighbourhood planning and operation. With Ravneberget as a case study, the interplay of PV generation, a shared EV pool, and operational energy demand is assessed in terms of selected key performance indicators. A finite set of likely combinations for EV charging are investigated to see how the neighbourhood's energy and emission performance can be affected by demand side management of EV charging. Further, implementation of peak shaving, with three different ambitions for storage level, is investigated for the selected performance indicators. Energy simulation outputs were used for building and mobility operations, and a binary search technique was used in the implementation of peak shaving. *Python* programming language was used for numerical tasks.

The results show that different combinations of EV charging gives different energy and emission performance for the neighbourhood, and especially for the emission calculations, the variation among the EV charging combinations are significant. The peak shaving improves the overall energy performance of the neighbourhood, but at the cost of higher emissions due to storage applications. Critical parameters are the emission intensity of electricity and emissions associated to material emission in PV panels and storage components. This work provides new research to the field of zero emission neighbourhoods and may be useful in neighbourhood planning and operation.

Sammendrag

Reduksjon av klimagassutslipp for å redusere klimaforandinger vil kreve store energi- og klimagassutslippsreduksjoner i bygningsmassen og mobilitetssektoren. Utviklingen av nullutslippsnabolag er en respons på slike tiltak. I dette studiet utvikles en metode som kan brukes i prosjektering og styring av nabolag. Med Ravneberget som case-studie har samspillet mellom solenergi, bildelingspark og energibruk i bygninger, blitt studert med hensyn på ulike ytelsesindikatorer. Et eksakt antall av sannsynlige ladekombinasjoner for nabolagets bildelingspark er studert for å se hvordan energi- og klimagassutslippsprestasjon påvirkes ved styring av elbillading på etterspørselssiden. Videre er kutting av effekttopplaster implementert, med tre ulike ambisjonsnivå for lagringskapasitet, og studert for de utvalgte prestasjonsindikatorene. Simuleringer av ett bygg og lading av en elbil ga grunnlaget for nabolagets energibehov, og binærsøk ble brukt for å implementere kutting av effekttopper. Programmeringsspråket *Python* ble brukt for numeriske oppgaver.

Resultatene viser at for ulike ladekombinasjoner av elbiler er energi- og utslippsnivåene forskjellige, med spesielt store variasjoner for klimagassutslipp. Kutting av effekttopper øker prestasjonsnivået med tanke på energi, men på bekostning av økte utslipp. Kritiske parametere er utslippsintensiteten for elektrisitet og utslipp i forbindelse med materialer i solceller og lagringskomponenter. Dette arbeidet bidrar til ny kunnskap i forskningsmiljøet for nullutslippsnabolag, og kan være nyttig i planlegging og styring av nabolag.

Contents

List of Figures

List of Tables

ARTICLE

Environmental science

Energy and GHG emission performance profiles at Ravneberget in Bergen – The interplay of onsite PV generation, electric vehicles sharing and battery storage for power peak shaving.

Marie Karvel Kyllingstad[1*]

[1]Department of Energy and Process Engineering, Industrial Ecology Programme, Norwegian University of Science and Technology (NTNU), Trondheim, Norway

Correspondence
Marie K. Kyllingstad, NTNU, Trondheim, 7030, Norway
Email: mariekky@stud.ntnu.no

In this study we develop a methodology that can be used in neighbourhood planning and operation. With Ravneberget as a case study, the interplay of PV generation, a shared EV pool, and operational energy demand is assessed in terms of selected key performance indicators. A finite set of likely combinations for EV charging are investigated to see how the neighbourhoods energy and emission performance can be affected by demand side management of EV charging. Further, implementation of peak shaving, with three different ambitions for storage level is investigated for the select performance indicators. Energy simulation outputs were used for building and mobility operations, and a binary search technique was used in the implementation of peak shaving. The results show that different combinations of EV charging gives different energy and emission performance for the neighbourhood, and especially for the emission calculations, the variation among the EV charging combinations are significant. The peak shaving improves the overall energy performance of the neighbourhood, but at the cost of higher emissions due to storage applications. Critical parameters are the emission intensity of electricity and emissions associated to material emission in PV panels and storage components. This work provides new research to the field of zero emission neighbourhoods, and may be useful in neighbourhood planning and operation.

KEYWORDS

LCA, peak shaving, zero emission neighbourhoods, EV pool, PV, multi-criteria decision support, demand side management

1 | INTRODUCTION

The central aim of the Paris Agreement is to hold the global average temperature increases to well below 2°C compared to pre-industrial times, contributing to increased focus on global climate change mitigation. Energy and emissions from the built environment, referring to buildings and transportation sector, were in 2017 accounting for 58% of the final energy use and 51% of the total emissions [3]. Residential buildings were responsible for 22% of the global energy use and 17% of the global CO_2 emissions. As buildings and transportation represents a critical part in a low-carbon future society, the interest in mitigation in these areas have lately increased, as implementations of mitigating measures are crucial in reducing impacts [4]. Moreover, buildings and infrastructure have long lifespans, and in order to avoid significant lock-in risks regarding long lasting technology solution choices, an urgent adaptation of state-of-the-art performance standards is necessary, both in renovation and in new-built [5, 6]. In order to achieve a highly energy efficient and decarbonised building stock by 2050, the EU has established a legislative framework that includes the Energy Performance of Buildings Directives (EPBD) and the Energy Efficiency Directive, specifying that by the end of 2020 all new buildings shall be "nearly zero energy buildings" [7].

In 2018, there was almost a doubling of new electric car sales compared to the previous year, with Norway as the global leader in terms of electric car market share [8]. Moreover, the overall electrification is increasing the annual electricity demand [9], and in particular is the penetration of electric vehicles (EVs) and photovoltaic (PV) panels in residential buildings imposing intra-daily fluctuations [9]. A drawback of renewable energy sources is that they are non-dispatchable, and must therefore be met by a local demand, exported to the external grid, or stored. Demand Side Management (DSM) is essentially the concept of improving the energy system at the demand side by load shifting [10]. DSM could be performed by load-limiters and smart metering [11], and further in combination with battery storage, to increase energy performance and flexibility. Self-consumption (SC) of PV generation is defined by Luthander et al. [12] as the self-consumed part relative to the total PV production, and self-sufficiency (SS) is the degree to which the PV power is sufficient to fill the needs of the energy demand in the building or neighbourhood [12]. EV home charging may have significant impact on such energy performance indicators. Assessing the energy and emission performance of a neighbourhood with EVS, in terms of a finite set of key performance indicators (KPIs) is necessary to prevent unfeasible design choices at the early development stages. Finding charging patterns of EVs with good performance with respect to a set of KPIs, must therefore be investigated as a multi-criteria decision making (MCDM) problem, which is the overall objective of this study. Developing such a tool would be useful in neighbourhood planning and DSM.

Lately, the focus has to some extent shifted from a building to a neighbourhood perspective [13, 14, 15, 16]. In extension of the Norwegian Research Centre on Zero Emission Buildings (ZEB Centre), providing information and recommendation of existing and new buildings [17], the Research Centre on Zero Emission Neighbourhood (FME ZEN) in Smart Cities was in 2018 conducted to develop cost and energy efficient neighbourhoods based on life cycle design strategies with no greenhouse gas (GHG) emissions, contributing to a low carbon society [18]. By using Life Cycle Assessment (LCA), a common and well-established tool, one can analyse environmental impacts of a product or process throughout its life cycle. The international standard ISO 14040:2006 [19] describes these principles and frameworks, providing a basis for comparing different sets of technologies and products, identifying environmental bottlenecks and integrating a life cycle perspective as a decision-support tool [5]. LCA has increasingly been used to evaluate the environmental impacts of buildings [20, 21, 22, 23], mobility service and batteries [24, 25, 26], energy storage solutions [27], and more lately in neighbourhood planning and assessment [13, 14, 28, 29]. Understanding that the goal and scope, assumptions (e.g. service lifetime of components, efficiencies, emission intensities etc.) and inventories vary amongst LCAs, are crucial in comparison of different studies.

1.1 | Environmental research

ZEBs are producing enough renewable energy to compensate for the buildings GHG emissions over its lifespan [17]. In Norway, the different ambition levels are defined according to the national standards NS3720 [1], stretched out in two dimensions to cover both physical elements and the life cycle modules included in the LCA. The ambition levels contain requirements for meeting a desired level, and range from ZEB O, including that the renewables are compensating for operational emissions only, to the most ambitious, ZEB COMPLETE, where the building's renewable energy production compensate for emissions throughout the lifespan, including building materials, construction, operation and demolition [17]. In extension, a similar modular structure for LCA modelling of ZENs are proposed by Lausselet et al. [28], with additional physical elements such as mobility, open spaces and infrastructure. These elements create systems with a greater scope and complexity, resulting in more heterogeneous approaches in LCA modelling on neighbourhood level compared to building level [29, 30]. In the research of LCA modelling of ZENs in early stage planning, buildings and mobility are found to account for 52% and 40% of the total emissions, with an ZEN OM ambition level [28]. This is supported by other literature, finding that buildings and mobility are the major contributors to primary energy consumption in the built environment, and that the embodied emissions in neighbourhoods can be of the same order of magnitude for highly energy efficient buildings [16]. As the literature on LCA on neighbourhood level is limited, more research and studies should be conducted to obtain consistent and robust methodologies and definitions. In particular, research regarding the neighbourhood mobility dynamics is poorly understood and requires further research.

The use phase emissions from mobility in neighbourhoods are significant, found to lay in the range of 44-57% [31, 32]. Lately, increased parking prices and reduced availability, decreases the demand for private vehicles in urban areas [33], and the literature agrees that car-sharing facilitates a car-free lifestyle, reducing the car-ownership and miles travelled, as the vehicle is provided in situations where it is actually needed [34, 35, 36]. Furthermore, a shared car is found to substitute 5-10 private vehicles and carpool members drive one third less than private car owners, reducing the need for privately owned cars [33]. Moreover, the literature address that private vehicles are parked on average 93 to 96% of their lifetime, hence a shared carpool could reduce the time the EV is an idle asset [37]. In extension, a shared carpool can be used to test technology solutions as Vehicle-to-grid (V2G) in neighbourhoods.

EVs displace petroleum use by using low-carbon or carbon free sources of electricity. The increased EV share of cars may have a significant impact on the capacity required by the grid in terms of adequacy and quality of the power supply, risk of supply, and costs [8], and the changes imposed on the power demand makes several studies conclude to adopt smart charging methods [38, 39]. In particular, could simultaneous EV charging lead to problems like local overloading [40]. Concerns regarding the power supply in Norway have lately increased [41], and even if Norway could handle a relatively large transition to EVs, simultaneous charging in one area may create local challenges for transformers and cables in the distribution network [42]. Uncontrolled charging of EVs may increase the peak load by a factor of 8.5 [43], and with the deployment of an EV fleet in neighbourhoods, understanding and quantifying the consequences are necessary. Moreover, understanding the environmental burdens from the production of the lithium-ion battery (LIB), which is a unique storage component of EVs, is crucial in assessing the energy and environmental benefits of EVs in a life cycle perspective [44, 45, 46, 47].

There are numerous studies investigating the grid impact of home-charging of EVs [38, 48], investigations regarding EV loads and PV power production, such as vehicle-to-grid (V2G) technology [49, 50, 51, 52], and optimisation techniques [53]. Furthermore, the coincidence between power consumption and PV power production, and how this changes with the introduction of a home-charged EVs have been studied [37, 54], and that the time of *when* charging occurs during the day is crucial in emission calculations due to variations in the emission intensity of electricity [55].

A questionnaire on the Norwegian charging habits for EV owners shows that the most frequent charging occurs at home or at work, relying on slow chargers. Moreover, fast charging primarily takes the form of planned stops for long distance trips [56], and that 38% never use a fast charger [57]. The questionnaire concludes that the nighttime charging usually occurs at home, whereas daytime charging occurs at work, and that cars with larger battery capacity more likely charge during the night, and cars with smaller capacity charge during the morning and afternoon [57]. As the power demand is in general lower at nighttime [42], shifting the charging to nighttime would be favourable for the grid. Controlled charging, and limiting it to overnight and off-peak charging, would mean that even large deployments of EVs are unlikely to burden electric power systems [58, 59, 60].

Smart charging could also provide operating reserves and system flexibility [37], and is often recommended to enhance reliability and resilience of power grids [38]. Tummina et al. [61] finds that even if the PV generation exceeds the electricity consumption, only 29% of the PV generation is used onsite on yearly basis. Hence, PV and EV could potentially be important complements to each other in addition to other technologies as load shifting and electricity storage [37], dealing with overproduction in the local distribution grids and avoiding grid reinforcements [54]. Quantifying the variations in electricity use in such buildings is important for assessing the grid impact at the end-user level in the grid [37, 54, 62, 63], especially as both EV home-charging and PV power production are intermittent [54, 63, 64]. If matching the onsite PV production and the energy demand in buildings with EV charging, smart charging of EVs in ZENs can play an active role in improving the degree of SC and SS [37, 54], and the energy flexibility and of an area [42, 65]. Furthermore, to mitigate the negative influence on the power grid, one could implement a storage technology to reshape the fluctuating load curve from building and mobility operation and onsite energy production.

1.2 | Peak load smoothing, flexibility and storage

The interaction flexibility between neighbourhoods and the grid is an important characteristic [66], and in recent years the integration of energy hubs, involving heating/cooling, power generation and storage systems, and smart grids, are shaping a new form of energy system - Smart Multi-Energy Grids [32, 67]. This includes the ability to respond to signals from the grid (e.g. price or CO_2 intensity) and consequently to adjust load, generation and storage control strategies in order to achieve the best interests of the stakeholders involved. Optimising EV charging from an economic point of view is described in several studies [68, 69, 70], and through a vehicle-to-home technology, there can be obtained a cost reduction in terms of a unidirectional charging of the EV [69, 70]. Chiang et al. [71] outlined three basic requirements to consider energy usage of smart grid on the daily basis: (1) storage of unused renewable energies, (2) shaving peak power demand and (3) economic control of battery discharge into grid. Moreover, the V2G technology has mainly the following three purposes: (1) peak shaving in buildings and areas, (2): maximise self-consumption and (3) flexibility service to the grid [42]. V2G can be implemented in terms of optimisation of smart energy management systems [52].

The ability of stationary batteries to tackle the challenges of intermittent energy production and demand, hence bringing flexibility to electricity systems with variable renewable energy sources, are largely driving the growth of global power capacity of stationary batteries [72, 73]. However, studies on life cycle impacts of stationary batteries are limited [24, 26, 74], compared to the batteries used in mobility applications [31, 44, 65, 26]. The lithium-ion (Li-ion) batteries have gained ground in storage application, much because of their high energy density, and because of a discharge of more than 5000 times in the case of 80 % depth of discharge (DoD) [25, 75]. The Li-ion batteries are also replacing other batteries due to performance, durability, safety and less environmental impacts [76, 77]. Overall, literature provides a great consensus that the Li-ion battery is the most convenient in automotive terms, where the most used types are the lithium manganese oxide and the lithium ion phosphate [78, 79, 80]. Despite the large

variations in impacts calculated, the literature on LCA methodology agrees on the significant environmental impact from batteries in EVs [81, 82, 83, 84, 85, 86]. Battery life and capacity are key aspects for the wide adoption of EVs [87]. Both a high and a low state of charge (SoC) contributes to deterioration of the battery [88], affecting the state of health (SoH). SoC is the complement of DoD; as one increases the other one decrease. The SoC range for EVs are often cycled within 20%-100%, i.e. a DoD of 80% [89]. Material parameters and environmental conditions, as well as storage and cycling conditions, influence the battery lifetime and performance [88]. Shallow cycling of batteries at the average SoC of 50% and an operating temperature close to 25°C could double battery lifetime [90], and authors agree that with an optimal charging-discharging operation, battery lifetime is increased, meaning less replacement costs and emissions during the EVs lifetime [49]. At present, a battery is considered reached end of life (EoL) when the battery capacity decrease to 80% of the initial rated capacity [44, 89, 91].

The emission factor, referred to as the emission intensity of electricity, is measured in g CO_2eq./kWh and its significance in emission calculations is discussed in several studies [21, 92, 93]. As the Norwegian power system is connecting to the Nordic, and with time to be fully integrated with the European, this should be reflected in the electricity mix [94]. For Norway, with an electricity mix of 10-15 g CO_2eq./kWh, a connection to the European grid, having an emission intensity of 361 g CO_2eq./kWh, indicates an increase in the electricity mix in Norway. Thus, implementation of onsite renewable and increased SC is therefore inevitable in decreasing the emissions from electricity consumption in a European perspective [95]. Furthermore, the emission intensity of electricity is a significant parameter in reducing the total GHG emissions from EVs [96], in particular in reducing the emissions from battery production, i.e. the embodied emissions [44]. Buildings with fluctuating self-generation, together with the emerging electric mobility solutions, are penetrating the residential built stock rapidly. Designing neighbourhoods in synergy with the grid, and to not induce additional stress on their functioning is necessary [97], and is motivating this study. This includes the interconnections between energy generation, demand, storage, and grid interactions.

1.3 | Problem statement

A comprehensive assessment of environmental impact, grid influence and self-consumption associated with battery energy storage (BES) solutions is missing in research. Moreover, these aspects were not considered under the advanced control strategies and the uncertain charging patterns. The overall objective of this MSc thesis is to examine a case neighbourhood with respect to the selected KPIs based on a finite set of likely combinations of EV charging profiles. The KPIs assessed are self-consumption (SC), self-sufficiency (SS), maximum grid load and emissions. In doing so, a methodology in order to understand and interpret neighbourhood performance in terms of KPIs may form a multi-criteria decision support tool. Furthermore, it will be investigated how peak shaving and energy storage affect the energy performance and emissions of a neighbourhood, including the interacting subsystems such as building demand, mobility needs, onsite energy generation, local energy storage, and import/export to external electricity grid. With a focus on EV charging profiles and the emissions from ZENs applying these strategies, the following research questions are being asked:

1. How does a finite set of neighbourhood load profiles give different results for the given KPIs, and which profiles are desirable?
2. How are the KPIs affected when implementing peak shaving strategies?
3. What are the critical factors that affect these contributions and what are their sensitivity?
4. What are the strengths and weaknesses of the methodology developed? How can it provide useful inputs in decision making and in neighbourhood planning and operation?

Section 2 provides the methodology and necessary data requirements and underlying assumptions, followed by the Results in Section 3. The findings are finally discussed and concluded in Section 4 and 5. Supplementary materials are referred to in the text and are to be found at the end of this paper.

2 | METHODOLOGY

Ravneberget, a joint project between the engineering consultant company, Sweco, and the local power company in Bergen, BKK, is a neighbourhood in the early planning phase, and will be located at Ravneberget in Bergen. Ravneberget will be used as case study with the conceptual design proposal taken as a starting point [98]. The methodology consists of five steps. In order to investigate how the energy and emission performance is influenced by the implementation of peak shaving in step five, step four is repeated. Figure 1 illustrates the work flow. Analytical tasks were carried out in Python using a set of libraries described in Supplementary Material S4.

1. Developing a model of a building unit that has the properties of a planned building unit
2. Simulating energy demand and PV generation of the unit followed by upscaling the results to a neighbourhood
3. Estimate a large number of likely cumulative energy demand patterns caused by the EV park
4. Compute and analyse a set of Key Performance Indicators (KPIs)
5. Develop and analyse the output of a set of peak shaving strategies

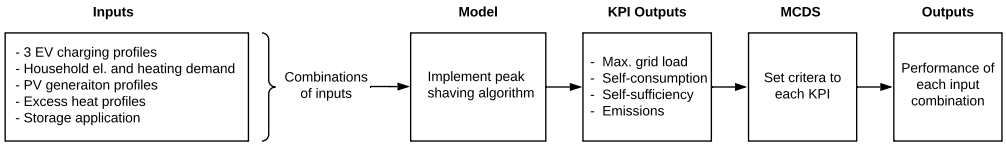

FIGURE 1 A schematic of the main modelling elements, including the input and output parameters used.

2.1 | Zeb Demo Building

The selected housing unit is a two-story, three-bedroom single-family house, based on the work in the MSc thesis of Maren Ingebretsen [99], further developed and adapted in collaboration with Sweco to fit the project characterisation. The model used in simulations is a housing unit in a vertical split, located at the end of a terraced building (to represent the worst-case scenario), built according to the Norwegian passive house standard NS3700 [100]. The heated floor area of the building unit modelled is 122.3 m^2 and each unit holds 2.6 people. The energy supply solution consists of district heating and solar collectors to cover heat and hot water supply, excess heat from a power transformer laying close to the neighbourhood, and electricity for lighting and electrical appliances is covered by PV panels and interactions with the electricity grid. See S1 in supplementary material for further explanations. The building unit's energy demand include space heating, domestic hot water (DHW), auxiliary heating unit (AHU), lighting and electrical equipment. The energy simulation program IDA ICE is used to simulate the units performance over a year, using the ASHRAE IWEC database with "typical" climate data for Bergen [101]. The energy performance simulation output is

scaled up to 130 buildings, giving 15899 m^2 heated floor area for the neighbourhood. Further details on building unit specifics, electricity and heat related assumptions are found in Supplementary Material S1.1.

2.2 | Mobility service and EV charging

The mobility service at Ravneberget is to be satisfied from sufficient public transport, good walking and biking facilities and a car sharing pool consisting of EVs. It is assumed that one shared car substitutes five private owned cars, and based on statistics on annual travel length and car ownership [102, 103, 104], the number of cars in the carpool is 36. This implies an annual travel length of 37 150 km/car, see S2 for calculations. Assuming an average energy consumption of 0.2 kWh/km [87, 105], the annual energy consumption per EV for charging is calculated to be 7430 kWh, an average of 20.5 kWh/day. The weekday:weekend ratio is 1.2:1, based on literature [42, 106]. The charging profiles for the EVs are further elaborated on in the following section. Figure 2 shows the distribution of energy use by buildings and mobility disaggregated by end users.

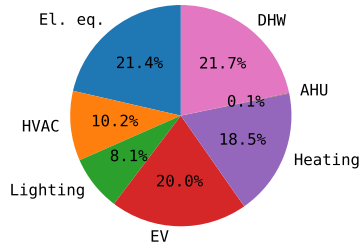

FIGURE 2 Annual operational use divided in percentage of the total.

Charging profiles

Three different EV charging profiles are used as input to generate the different aggregated neighbourhood EV charging combinations. For each combination, the KPIs to be described in Section 2.4 are calculated, with a goal of addressing which neighbourhood charging combinations that are desired. The EV charging profiles are suggestions and are chosen to investigate the KPIs under different time-of-use periods where the results can be used for DSM. The charging profiles are listed below, and Figure 3 illustrates the energy demand for each profile for a given day and week:

- **EV1:** Charging profile 1 (EV1) is based on data from a questionnaire among EV owners, following the charging data from the Tesla model S sample [42]. The main charging occurs during night, morning and evening with less charging during midday, often common for charging of larger battery packs [57].
- **EV2:** Profile 2 (EV2) has the charging demand split between 10 hours, i.e. 9 pm and 6 am.
- **EV3:** Profile 3 (EV3) has the charging split between 6 hours, i.e. 10 am and 4 pm. The total demand remains at 20.5 kWh per vehicle and day for Profile 2 and 3.

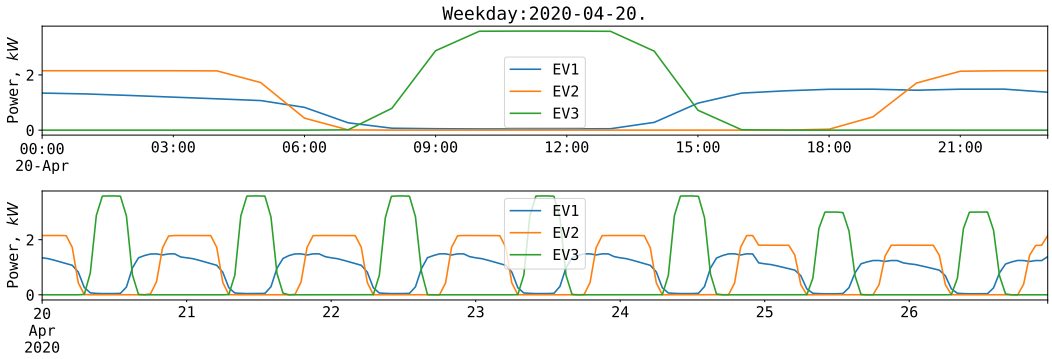

FIGURE 3 Energy demand per day and week for one EV, shown for the three charging profiles.

Given a set of size r where each element can have n possibilities, the total number of possible unique combinations of such a set can be computed as:

$$N = \frac{(r+n-1)!}{r! \cdot (n-1)!} \tag{1}$$

Having 36 (r) EVs with the possibility of charging with three (n) different schedules, the number of combinations, i.e. the number of multisets, yield 703 (N) unique neighbourhood charging combinations, see Equation 1 [107]. A multiset is intuitively a set with repeated elements, here charging profiles. Examples of four neighbourhood charging combinations are listed below:

Combination 1:	{1,1,1,$\cdots$,1,1,1}
Combination 2:	{1,1,1,$\cdots$,1,1,2}
Combination 3:	{1,1,1,$\cdots$,1,2,2}
Combination 703:	{3,3,3,$\cdots$,3,3,3}

The energy and emission performance for each of the 703 combinations is assessed in this study, first without peak shaving, referred to as "base case", followed by implementation of peak shaving with three different strategies, further explained in Section 2.3. Figure 4 shows the electricity demand when all 36 EVs charge with EV1, i.e. charging combination 1: {1,1,1,$\cdots$,1,1,1}, in addition to building heat and electricity demand, heat delivered from the transformer station and neighbourhood PV generation. The illustration shows a week in February, a typical representative week in a cold winter period. See supplementary S2.1, Figure S2.1 and Figure S2.2 for similar illustrations but for EV charging combination 666: {2,2,2,$\cdots$,2,2,2} and combination 703: {3,3,3,$\cdots$,3,3,3} respectively.

2.3 | Load matching

In order to rationally use all the PV generation locally, the energy must be stored and re-allocated to the time of the day where the energy demand is the highest. This way, high peak loads are avoided. The purposed algorithm implies that PV energy can be stored in batteries and used to cover peak loads that day. Further, we account for the possibility of peak load shaving though the longer period, for peaks that occur on a weekly (W) and monthly (M) basis, to address the

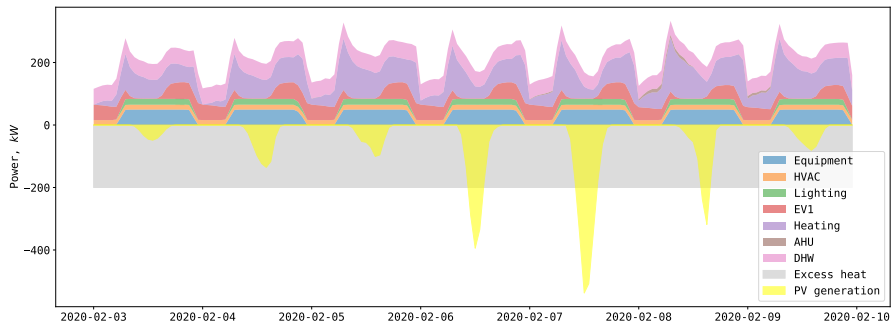

FIGURE 4 Neighbourhood energy load, heat supply and PV generation for a week in February, when all EVs charge with profile EV1.

benefits and drawbacks of different time periods related to the assessed KPIs. Equation 2 gives this energy balance, where usually the PV generation is less than the electricity demand, and a threshold must be found to satisfy the equation. To obtain the threshold p for which all load above this value is covered by the PV generation (drawn from storage units), and all load below this threshold is covered by electricity imported from the grid, a numerical search technique, in particular a binary search algorithm, has been implemented. The search process functions by trials and errors in a systematic way, exploring the continuous space by comparing the target value with the middle element of the search space, and eliminating half the continuous search space not containing the target value. The search process continues in the remaining space and is repeated until the target value is achieved. From knowing the total available PV generation, we achieve the threshold value separating grid load and battery load. Supplementary S4 Figure S4.1 proves a flowchart of a binary search.

$$\sum_{1}^{24} P_{PV} = \sum_{n=1}^{n} \left(\sum_{T_1}^{T_2} (P - p) \right) \pm \epsilon \tag{2}$$

$$\text{for all } (P - p) > 0 \text{ and } \sum_{1}^{24} P_{pv} > 0$$

P_{PV} is the hourly PV energy in kWh, P is the hourly energy use in the building including EV charging, ϵ is the absolute error tolerance, and $T_1 and T_2 \in [0, 24]$ is the beginning and end of interval n where the battery should be used. The algorithm is applied for peak load shaving on a daily (D) basis (as described above), weekly (W) and monthly (M) basis.

Figure 5 provides an example of the peak shaving strategy. Subfigure 5a illustrates the binary search process, and Subfigure 5b illustrates the reshaped grid interaction curve, also displaying the total energy saved, here 155 kWh. The neighbourhood threshold value on a given day is found to be 30.6 kWh (0.24 kWh per household) found after eight iterations. The total load above this threshold, i.e. the difference between the yellow and green lines in Subfig. 5b, will be covered by PV generation drawn from the battery in different intervals n. For a day where the PV production exceeds the daily demand, excess energy is exported to the grid, see Figure S4.2 in S4 as an example.

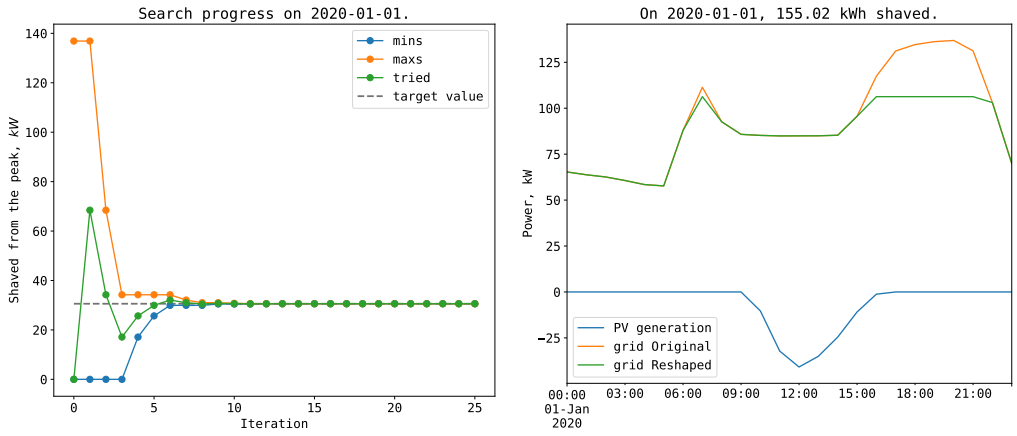

(a) Binary Search process.

(b) Reshaped curve for grid interaction.

FIGURE 5 Search process for battery storage with a daily peak shaving strategy on Jan. 1st.

2.3.1 | Storage

Simplified battery storage models are assumed in this work. Equation 3 describes the energy balance, Equation 4 is restricting the state of charge, and Equation 5 is limiting the maximum charge and discharge rates.

$$E_t = E_{t-1} \cdot Decay + \eta_{Charge} P_{Charge} \Delta T - \frac{1}{\eta_{Disharge}} \Delta T \tag{3}$$

$$E_t \leq Cap \tag{4}$$

$$P_{Charge/Discharge} \leq Cap \delta_{Charge/Discharge} \tag{5}$$

E_t is the storage level in the battery, $P_{Charge/Discharge}$ is the charge/discharge powers in kW, η are the efficiencies. It's assumed a Li-ion battery with charge/discharge efficiency of 100%, and a decay of 0% per hour [27].

Storage specifics

If a peak shaving strategy is implemented, the associated emissions from battery production are calculated and added to the neighbourhood emissions. The batteries are assumed to be 75 kWh Li-ion batteries as described in L. Vandepaer et al. [24]. The results from the LCA yields emissions of 130.73 kg CO_2eq/kWh storage capacity and a battery lifetime of 5000 charging cycles, based on a depth of discharge (DoD) of 80%. The storage emissions are calculated according to Equation 6:

$$E_{M,storage} = f_{battery} \cdot C_{installed} \cdot \frac{E_{TH}}{E_{LTcapacity}} \tag{6}$$

$f_{battery}$ is the impact per nominal installed capacity ($kgCO_2eq/kWh_{installed}$), $C_{installed}$ is the battery's installed capacity (kWh), E_{TH} is the energy stored in the battery over the time horizon analysed (kWh/TH), and $E_{LTcapacity}$ is the storage capacity over the lifetime of the battery (kWh/battery lifetime). The latter fraction, $\frac{E_{TH}}{E_{LTcapacity}}$, yields the total number of batteries required over the time period assessed, which is dependent on the installed capacity and the number of charging cycles until it reaches end of life (EoL).

2.4 | Key Performance Indicators

A set of KPIs are calculated to assess the neighbourhood performance. The load duration curve for positive values will show the the load for when the neighbourhood is importing electricity from the grid. The highest value, P_{max}, is the maximum grid load and is the first KPI. The next two KPIs are the SC and SS. By the definition of Luthander et al. [12] the SS is defined by Equation 7:

$$\varphi_{SS} = \frac{\int_{t=t_1}^{t_2} M(t)dt}{\int_{t=t_1}^{t_2} L(t)dt} \tag{7}$$

where $M(t)$ is PV energy used on-site and $L(t)$ is the instantaneous building power consumption. SC is defined by Equation 8:

$$\varphi_{SC} = \frac{\int_{t=t_1}^{t_2} M(t)dt}{\int_{t=t_1}^{t_2} P(t)dt} \tag{8}$$

where $P(t)$ is the instantaneous PV power generation. In the case of energy storage, where $S(t)$ is the energy flow into/out from the storage unit, $M(t)$ is expressed by:

$$M(t) = min\{L(t), |P(t) + S(t)|\} \tag{9}$$

with $S(t) < 0$ when charging and $S(t) > 0$ when discharging. The surplus PV power is used to the fullest extent, by matching the load as described in 2.3. Losses due to charging, storing and discharging are not considered. Even though the formulas call for continuous integration over the investigated time period, SC and SS are calculated using discrete data with an hourly resolution. The integration period is over a year to account for seasonal variations and minimise the influence of short-term fluctuations in generation and demand.

The neighbourhood emission calculations are based on the NS3720, and ReCiPe v1.12 is chosen for the midpoint category global warming potential (GWP100). The emissions are measured in kg CO_2eq. [1], and is the fourth and last KPI assessed in this study. Other impact categories are not considered. The period of analysis (POA) is set to 60 years, i.e. from 2020 to 2080. In a ZEN framework with a ZEN-OM ambition level, Equation 10 gives the total neighbourhood emissions, considering the material (M) and operational (O) life cycle stages for a neighbourhood with the following elements: Buildings $E_{B,M}$ and $E_{B,O}$, PV system $E_{PV,M}$, Mobility $E_{M,M}$ and $E_{M,O}$, Infrastructure $E_{I,M}$ and $E_{I,O}$, and storage components $E_{M,storage}$

$$E_{tot} = E_{B,M} + E_{B,O} + E_{PV,M} + E_{M,M} + E_{M,O} + E_{I,M} + E_{I,O} + E_{M,storage} \tag{10}$$

Including only the emissions related to operation and energy systems, the equation above reduces to Equation 11. Material emissions from buildings, mobility and infrastructure are therefore omitted.

$$\begin{aligned} E_{tot} &= E_{B,O} + E_{PV,M} + E_{M,O} + E_{M,storage} \\ &= E_{el,imp} - E_{el,exp} + E_{DH} + E_{PV,M} + E_{M,O} + E_{M,storage} \end{aligned} \tag{11}$$

$E_{B,O}$ is met by both electricity (el) and district heating (DH). Some of the electricity demand for buildings and mobility operation is also met by onsite PV production, where the building demand is first covered and then electricity demand for EV charging. How the onsite PV production is allocated is insignificant for the emission calculations, because the amount of electricity drawn from the grid is just the remaining electricity demand not covered by onsite production. $E_{M,storage}$ is zero for base case, i.e. when there is no peak shaving strategy implemented. The emission intensities of electricity are calculated based on NS 3720 [1], and a Norwegian (NO) emission intensity is used in this study. The emission intensity of the excess heat from the transformer station is assumed zero. The emission intensity of district heating is based on [108] and the 2019 declaration on District heating (provided in email correspondence with Martin Horne), with an average value of 157.83 g CO_2eq/kWh. The PV module emissions are 281 kg CO_2eq/m^2, in line with the literature finding these emissions in the range of 100-300 kg CO_2eq/^{2} [83, 109]. To account for the material emissions in the PV system, an intensity of 45 g CO_2eq./kWh is applied for the generation of energy. The intensity is assumed halved when the replacement occurs after a 30 years period, due to technical improvements. Further detailed description on the calculations and references used to obtain the evolution of electricity mix, emission intensity for district heating and PV can be found in S3.1 and S3.3 in supplementary material. Figure 6 illustrates the evolution of the emission intensities over the POA.

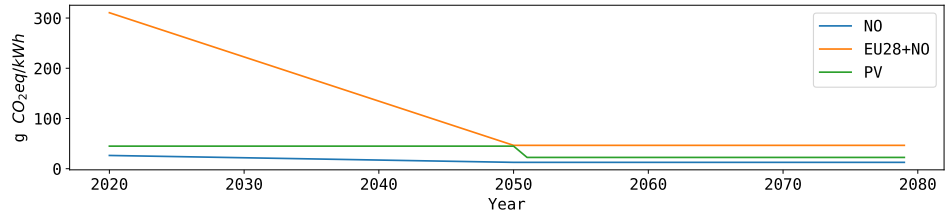

FIGURE 6 Evolution of electricity mix for the two Scenarios NO and EU28+NO suggested in NS3720 [1].

2.5 | Sensitivity analysis

To address the goal of assessing critical parameters in the energy and emission analysis, a sensitivity analysis is performed on parameters expected to have significant impacts on the results. The relative sensitivity tells us how a function change when there is a relative change in one parameter, and provides better understanding of the relationship between inputs and outputs of a model. The relative sensitivity to a function F to the parameter α, evaluated at the normal operating point is given by Equation 12:

$$\bar{S}(F,\alpha) = \frac{\%\ change\ in\ F}{\%\ change\ in\ \alpha} = \frac{\partial F}{\partial \alpha}\Big|_{NOP} \cdot \frac{\alpha}{F} \tag{12}$$

Equation 12 can be used to find the relative sensitivities of selected parameters on the four KPIs, and allows for comparing each parameters relative impact. In addition, the assumptions of the emission intensity of electricity and the allocation of emissions from the waste incineration at the district central energy plant, are expected to have a great impact on the results, and are therefore investigated. For the latter, an average value of 14.41 g CO_2eq/kWh is used when allocating the emissions from waste incineration to the waste producer, significantly lower than 157.83 g CO_2eq/kWh, which is used in this study.

3 | RESULTS

The results are first presented for the average KPIs, described in Section 2, among the neighbourhood charging combinations for the base case and each peak shaving strategy. The emission results are elaborated in detail and presented according to Equation 11, and are given as annual averages in kg CO_2eq/m^2 and year. The base case optimal charging combination for each KPI is addressed, illustrating the need for a multi-criteria decision support (MCDS) tool. Then, the MCDS tool is demonstrated with a set of example criteria in order to decide which charging combinations are desired in terms of the KPIs. Lastly, the sensitivity shows the change in the KPIs when there is a relative change in 25% for each parameter assessed.

Maximum grid load

The maximum grid load for all cases can be seen from Figure 7. The histogram clearly illustrates that the density of load among the 703 combinations is shifted to the left, when increasing the storage. However, for all PS scenarios the long tail shows that there will be certain combinations with a high maximum grid load. The load duration curve shifts down as the storage capacity increases. Table 1 provides the range for the maximum grid load for the different neighbourhood charging combinations, mean values, and the percentage changes of means from base case.

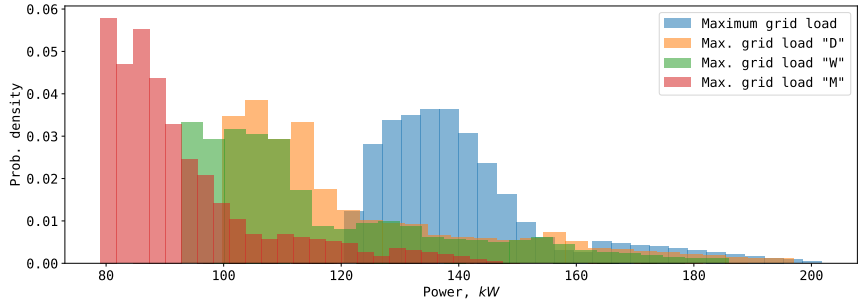

FIGURE 7 Maximum grid load for base case and for all peak shaving scenarios for all charging combination.

TABLE 1 Max grid load after implementing peak shaving strategy.

Scenario	Max. grid load range [kW]	Mean	Change from BC
Basecase	120.5-201.7	**141**	-
Peak Shaving D	99.8-197.0	**123.2**	-12.6%
Peak Shaving W	92.7-185.9	**116.2**	-17.6%
Peak Shaving M	79.1-147.7	**93.0**	-34.0%

Self-consumption and Self-generation

Figure 8 provides the mean SC and SS for base case and all peak shaving strategies. The increase in SC and SS from base case increases as the time perspective of peak shaving increases. Because the energy demand and PV production is similar regardless of charging combinations, the SC and SS is varying marginally among all 703 combinations. For the base case, these results reveals that midday charging, i.e. the EV2 profile, yields highest SC and SS, see Figure

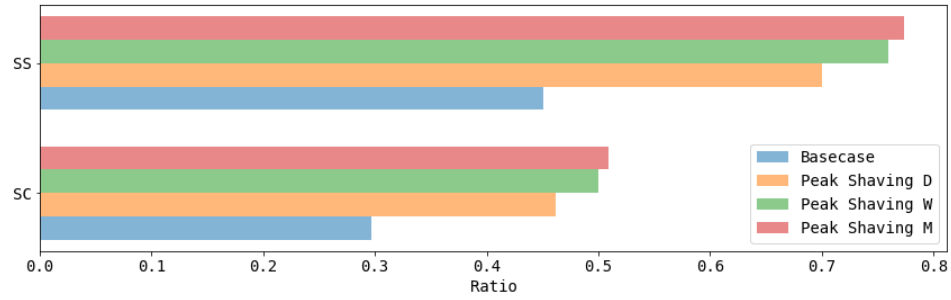

FIGURE 8 SC and SS average for base case and for the three peak shaving strategies.

TABLE 2 SC and SS after implementing peak shaving strategy.

Scenario	Self-consumption	Mean	Change from BC	Self-sufficiency	Mean	Change from BC
Basecase	0.24-0.38	**0.30**	-	0.36-0.58	**0.45**	-
Peak Shaving D	0.4613-0.4614	**0.46**	53.3%	0.7001-0.7004	**0.70**	55.5%
Peak Shaving W	0.50	**0.50**	66.7%	0.7589-0.7591	**0.76**	68.9%
Peak Shaving M	0.5094-0.5095	**0.51**	70.0%	0.7731-0.7734	**0.77**	71.1%

10, and Figure S5.5 in Supplement S5.2 illustrates the the top ten EV charging combinations. Table 2 provides the ranges of SC and SS for the neighbourhood charging combinations, mean values, and percentage changes of means from base case.

Emissions

Figure 9 provides the results for the mean total emissions for base case and for all peak shaving strategies, distributed between elements and life cycle stages. The net emissions are given by the dotted lines after subtracting export of onsite PV generation. Because building energy demand is first covered by onsite PV generation, these emissions are very low for base case. When implementing peak shaving, the SC is so high, that the entire building demand is covered as well as parts of the mobility demand. In general, the embodied emissions in PV panels are accounting for most of the emissions, and PV exports are not compensating for the embodied emissions in the panels. Due to utilisation of excess heat from the power transformer, marginal emissions come from district heating. The increase in emissions from base case increase as the time perspective of peak shaving increases, due to higher storage requirement, thus increased emissions from batteries. As more energy is self-consumed, less energy is exported, see Supplementary S5.3 Table S5.1 for further details. Table 3 provides emissions for each case, and the percentage change in emissions from base case. The total emissions over the POA are found to be 1.0 kt CO_2eq for base case, and 2.6, 2.7 and 2.8 kt CO_2eq for D, W and M peak shaving strategy respectively. The results show that the emissions among the different charging combinations are varying more when implementing a peak shaving strategy, than for base case, see S5.3 Figure S5.6. Hence, the importance of charging strategy for the neighbourhood increases as peak shaving is implemented. Charging with EV1 yields the lowest emissions, see Figure 10. Figure S5.7 in Supplementary S5.3 illustrate the top ten combinations of EV charging.

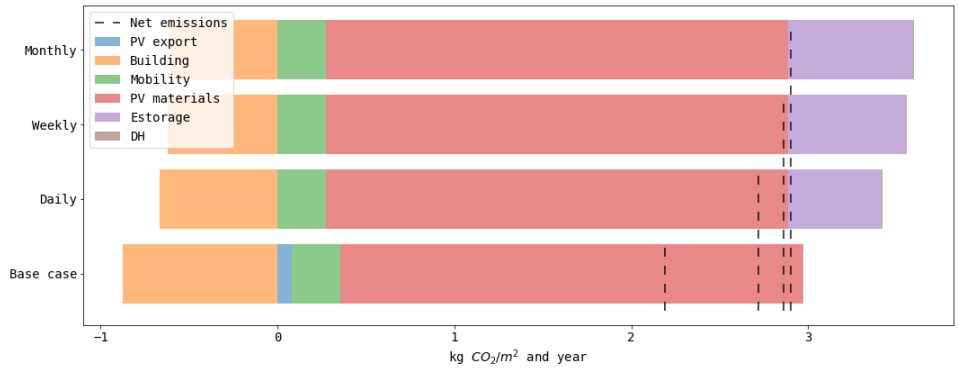

FIGURE 9 Neighbourhood emissions for all cases in kg CO_2eq/m^2 and year distributed between elements and life cycle stages.

TABLE 3 Total emissions after implementing peak shaving strategy.

Scenario	Emission range [kg CO_2eq/m^{2}yr]	Mean	Change from BC
Basecase	2.193-2.194	**2.194**	-
Peak Shaving D	2.556-2.842	**2.722**	+24.1%
Peak Shaving W	2.732-2.952	**2.858**	+30.3%
Peak Shaving M	2.779-2.987	**2.899**	+32.1%

If the controlled charging were based on each of the KPIs, the neighbourhood would perform poorly in each of the other KPIs. The best charging combinations for base case, as explained for each KPI, are illustrated in Figure 10, illustrating the significant different optimal charging solution when satisfying only one criterion. Hence, the need for a tool covering all aspects, i.e. a multi-criteria decision making tool is developed.

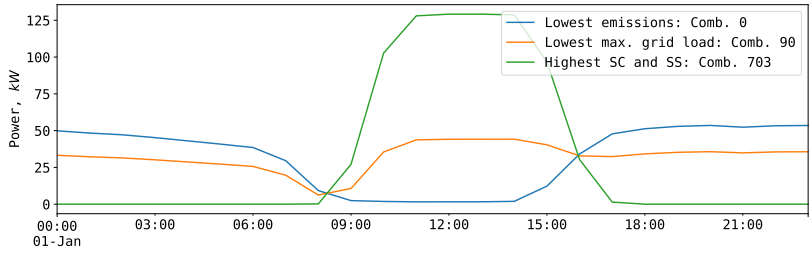

FIGURE 10 Optimal neighbourhood charging combinations for base case, with respect to each KPI.

Figure 11 shows the KPIs for the three ambitions of storage, for all charging combinations of the EV fleet. It can be observed that the desired degree of SC, SS and maximum grid load comes at the cost of higher emissions. Speaking in energy performance terms, a peak shaving strategy with storage over a month is desired. However, the emissions are higher compared to a shorter storage ambition.

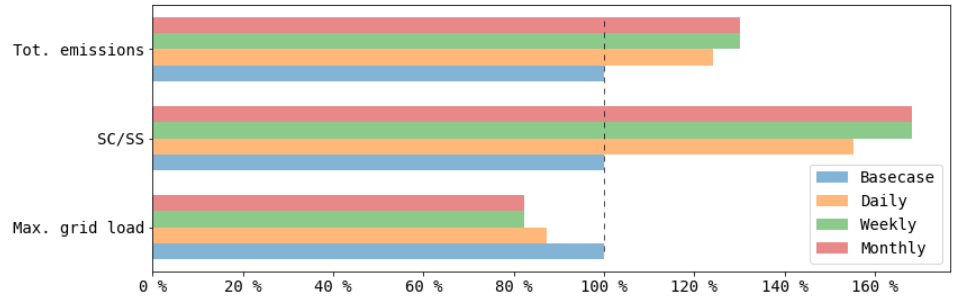

FIGURE 11 Summary of the KPIs for all combinations when peak shaving is implemented.

Storage perspectives and requirements

Table 4 shows the storage capacities required by the neighbourhood and for each household, as well as the number of batteries per year and over the POA in parenthesis. The number of batteries are calculated with the assumptions on batteries described in Section 2.3.1. Note that because of a higher peak storage requirement with a weekly storage perspective compared to the monthly storage perspective, the storage capacity must be larger for the former. However, due to larger amount of stored energy with the monthly strategy, the total number of batteries are higher, which is also the reason for higher associated emissions for this peak shaving strategy, compared to the other two.

TABLE 4 Storage requirement for different ambition levels.

Storage strategy	Storage Cap./Neighb.	Storage Cap./Household	# batteries/Neighb. and year (POA)
Daily	656 kWh	5.04 kWh	0.857 (51.4)
Weekly	1230 kWh	9.46kWh	1.076 (64.6)
Monthly	1167 kWh	8.97 kWh	1.144 (68)

Figure 12 illustrates the neighbourhood power demand and PV output curves for daily storage ambitions, for charging combination one. For days when consumption exceeds generation, the latter is entirely matched to the upper part of the power demand. The remaining energy, shaded in purple, is covered by grid import. Contrary, the sea green shaded area is grid export, when generation exceeds consumption. The expected battery behaviour during the same period, is shown in Figure 12 b. The week displayed is chosen to illustrate both import and export.

Due to little seasonal variation in electricity demand, because seasonal variation mostly varies with delivered heat, which in this neighbourhood is delivered by district heating, the charge/discharge curves among the storage strategies varies little. The main difference is that for days with high PV production, the daily strategy will have larger exports, whereas for strategies with a longer time frame, more energy will be stored in the batteries. The opposite happens if the energy demand is high, the daily strategy requires more electric import, whereas the peak shaving with longer time frames draw more from the batteries. See Supplement S5.4 for similar graphics for weekly and monthly strategies.

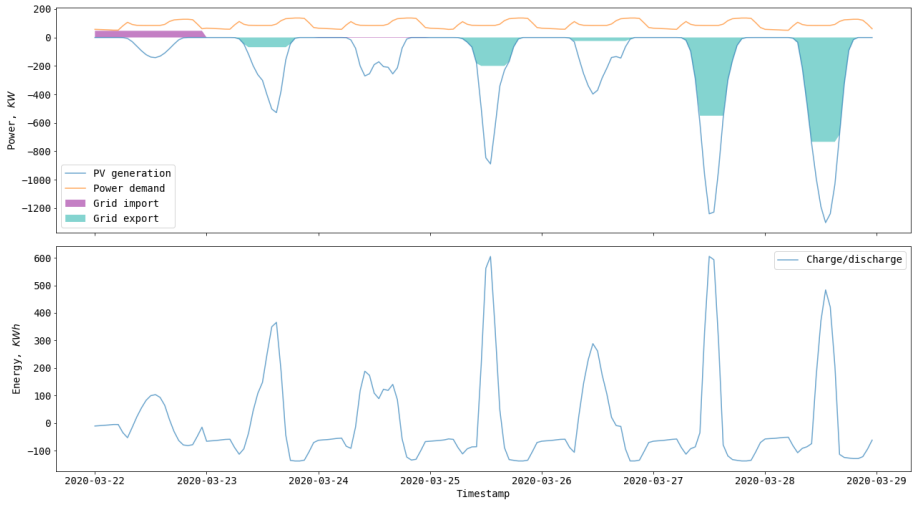

FIGURE 12 Charging combination one: (a) Energy consumption and production and grid interaction: (b) Battery charge/ discharge dynamics.

3.1 | Decision support tool

In order to understand and interpret neighbourhood performance in terms of all KPIs, an illustration showing the relationship between the KPIs are needed. In order to validate if a charging combination is desired or not, criteria may be set to classify the performance of each of the 703 charging combinations. Table 5 provides an example of how these criteria can be set, with proposals for restrictions on each of the KPIs, implemented to evaluate the energy and emission performance of each combination. The SS vary marginally among the peak shaving strategies, see Table 2, and is not included as a restriction in the MCDM tool. The SS varies more among the combinations for base case and could thus be considered as a fourth restriction if it is desired to explore this aspect. A charging combination is valuated as "Good (G)", "Medium (M)" or "Poor (P)", depending on which criteria that are satisfied for the different KPIs. Two proposals for restricting the emissions are given in Table 5, to illustrate that the number of G, M and P combinations changes according to changes in the criteria. As a proposal to how the decisions of which EV charging combinations are desired for the neighbourhood, thresholds were set according to a trial and error procedure in order to exemplify the decision process. This replicate what could happen in a real decision making process, where stakeholders would set thresholds in order to satisfy criteria for each KPI as they please. All "means" used as restrictions, are calculated for the respective scenarios assessed, i.e. base case, peak shaving with D, W and M strategy.

TABLE 5 Example of criteria used in decision making.

KPIs	Good	Medium	Poor
Max grid load	< 0.95 · mean	< 1.05 · mean	all other
SC	> mean	> 0.95 · mean	all other
Total emissions (1)	< mean	< 1.05 · mean	all other
Total emissions (2)	$< Emax_{limit}$	$< 1.05 \cdot Emax_{limit}$	all other

** where $Emax_{limit}$ = 2.85 kg CO_2/m_2 yr

Figure 13 shows the pair plot for base case. The green, yellow and blue dots represents G, M and P performance respectively, based on the restrictions in Table 5 and emission restriction number one. The diagonal elements in Figure 13 shows the distribution of each KPI for all charging combinations (the kernel density estimates), and the off-diagonals illustrate the relationship between two KPIs for all charging combinations. For instance, the lower right corner shows the smoothed distribution of the emission performance for all charging combinations. It illustrates the distribution of performances, i.e. G, M and P, for all emission estimates for the charging combinations. Note that the emissions vary marginally for the base case, and therefore, the minimum value has been subtracted from the emissions for illustrative purposes. The emissions are still in the range as displayed in Table 3. Assessing the relationship between two variables, e.g. emissions and SS, the emissions does not change significantly when increasing the SS. Contrary, there is clearly a linear relationship between SS and SC, illustrating that for an increased SS the SC also increase. The pair plot illustrates that the KPIs must lie within a certain range in order to satisfy the criteria for the performance categories. With the example criteria, the pair plot reveals that the SC and SS, emissions and max grid load, must have values concentrated around 0.32, 0.49, 2.194 kg CO_2eq/m^2 and year and 140 kWh respectively. The charging combinations which satisfy the G performance critera are combinations with night and evening charging for base case, a mix of day- night- and midday charging for daily and weekly strategies, and for monthly, combinations of night- and midday charging. Supplementary S5.6 provides graphics for G, M and P charging combinations for base case and all peak shaving strategies, obtained by the pair plots. The number of combinations satisfying the G performance critera are 77, 8,9 and 18 for base case and D, W and M peak shaving strategies respectively, and it is the maximum grid load criterion which is limiting the number of good combinations for the peak shaving strategies. Further detail on these results are to be found in S5.6.

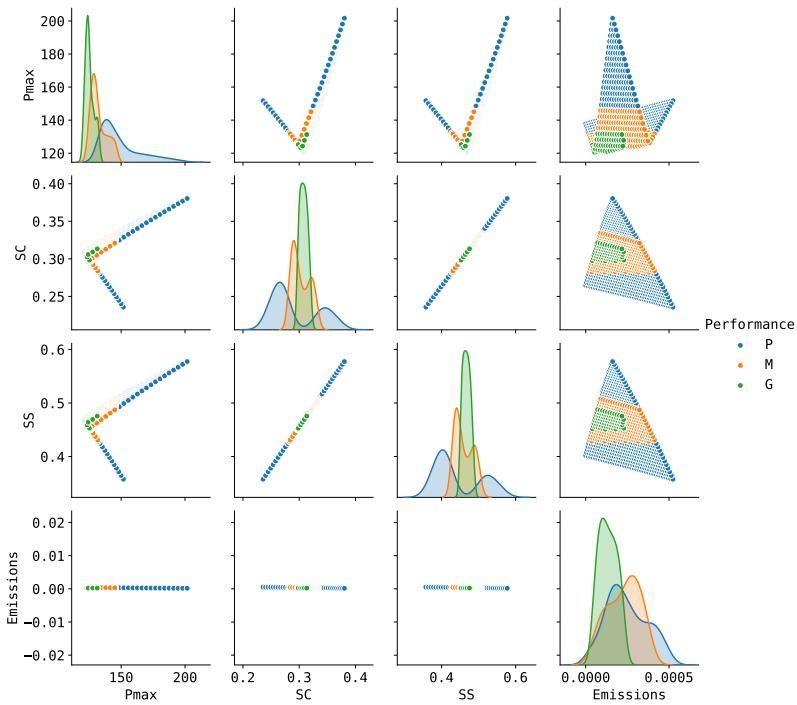

FIGURE 13 Pair plot of the KPIs for base case, with mean emissions restrictions.

The emission criterion can also be set according to a finite limit, e.g. 2.85 kg CO_2eq/m^2 and year as shown in Table 5, and as a result, the composition of performance changes. For base case, Figure 14 illustrate that the number of charging combinations satisfying the G performance criteria increases, whereas for weekly peak shaving, see Figure 16, there are zero combinations satisfying the G performance criteria. For the daily and monthly storage perspective, pair plots illustrating both emission criteria are to be found in Supplementary S5.3, Figure S5.10 and S5.11, and Figure S5.12 and S5.13. Changing the emission criterion from one to two yields no change in G performance for D strategy, and zero combinations with G performance for monthly strategy. The pair plot illustrates how the different KPIs must lie within a range to satisfy a certain performance. For instance, a charging combination with high SC would be at the cost of decreased performance of other KPIs, giving a M or P overall performance. The tool is adaptive to reflect any of the design option considered by the stakeholders, by specifying the criteria in Table 5 as desired.

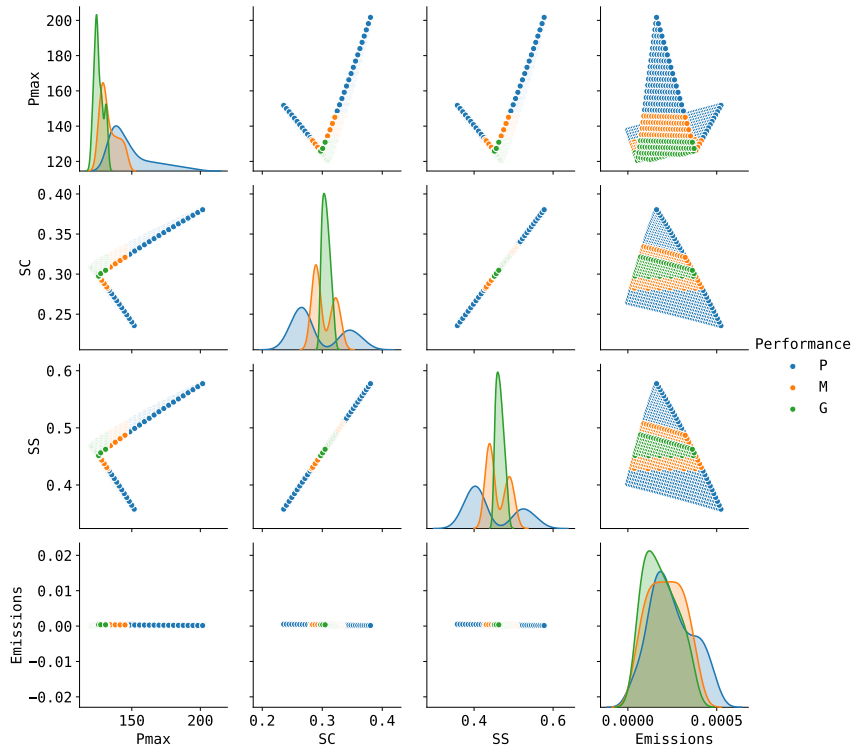

FIGURE 14 Pair plot of the KPIs for base case, with E_{max} restriction.

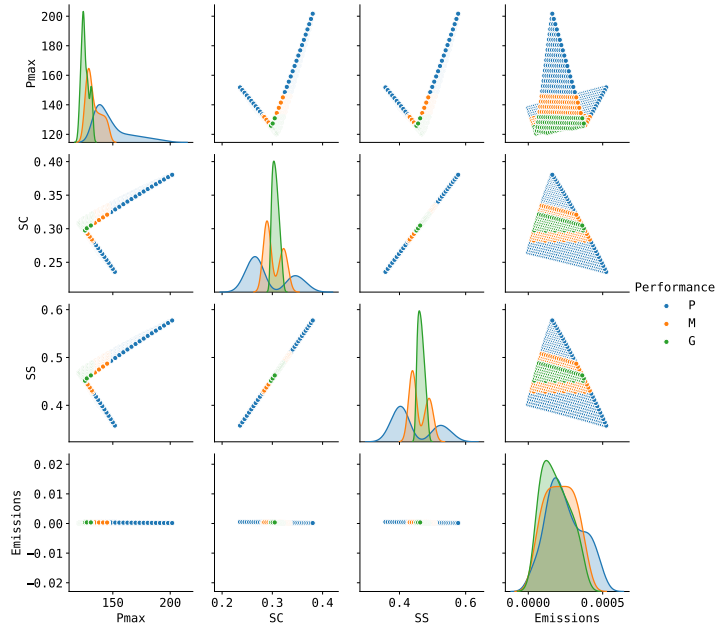

FIGURE 15 Pair plot of the KPIs for weekly peak shaving strategy, with mean emissions restrictions.

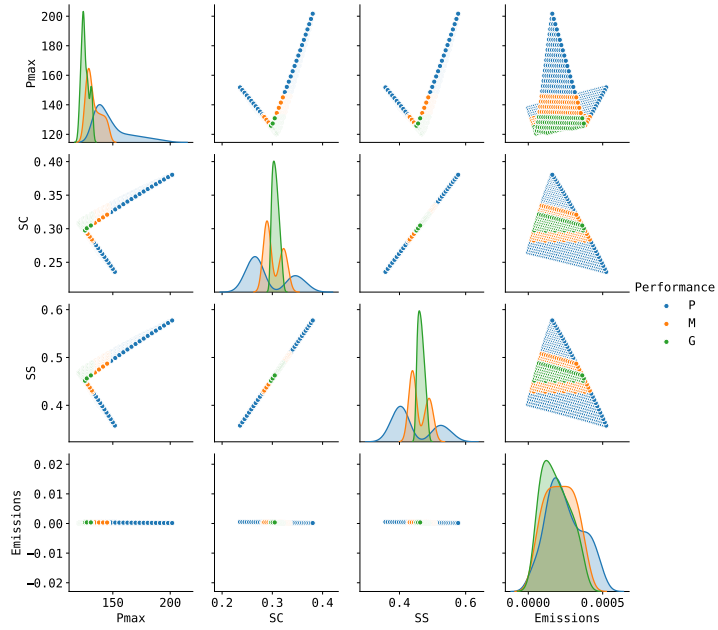

FIGURE 16 Pair plot of the KPIs for weekly peak shaving strategy, with E_{max} restriction.

3.2 | Sensitivity analysis

The sensitivity analysis and the change in the KPIs are shown in Table 6. In general, the results show that the KPIs are sensitive to changes in all parameters, except emission intensity of district heating due to little delivered district heat. Although the increased PV area increase the SC, the associated emissions increase with around 14-15% due to embodied emissions. When changing the PV area size, we see that the SC is lowered because whenever there is excess energy from onsite PV production, the exported energy gets even larger. The SS increase because a larger share of the neighbourhood energy demand is now fulfilled by the onsite generation. When increasing the EV travel length by 25%, i.e. the total energy associated with EV charging increases from 20% to 23.8% of the total neighbourhood energy consumption. Further details are provided in Supplementary S5.7.

TABLE 6 Results sensitivity for selected parameters.

	% change in Avg. Max. grid load				% change in Avg. SC/SS				% change in avg. missions			
Sensitivity Parameter	BC	D	W	M	BC	D	W	M	BC	D	W	M
Emission intensity of el. +25%	-	-		-	-	-	-	-	-7.9	-6.3	-6.0	-6.0
Emission intensity of DH +25%	-	-		-	-	-	-	-	0.05	0.04	0.03	0.02
Charging cycles +25%	-	-		-	-	-	-	-	-	-3.9	-4.6	-4.9
Emission intensity of storage +25%	-	-		-	-	-	-	-	-	4.9	5.8	6.1
Area of PV panels +25%	-0.6	-2.1	-2.7	-6.4	-16.2/4.8	-15.7/5.1	-16.5/4.4	-16.4/4.4	15.6	14.6	14.4	14.3
Energy load (el. and heat) +25%	15.1	16.6	17.6	21.7	13.9/-2.3	11.2/-4.7	12.5/-3.5	12.6/-3.4	6.2	6.4	6.5	6.6
Excess heat supply +25%	-	-	-	-	-	-	-	-	4.7	3.8	3.6	3.5
Travel length of EV +25%	10.6	11.0	10.7	11.1	4.8/-3.3	5.7/-2.5	6.4/-2.9	3.6/-1.9	3.1	3.6	3.5	3.7

Figure 17 reveals that the emission intensity of electricity is significant in emission calculations. Due to large PV production and export of excess energy, a high emission intensity as in the EU28+NO scenario yields lower emissions, despite the fact that the operational emissions increases. The emissions for all four cases are reduced with a European mix, compared to the Norwegian. Sensitivity on District heating intensity, with and without the supply of excess heat from the transformer, is included in Supplementary S5.7. The results reveal that for a neighbourhood with excess heat supply of this scale, the heat demand is so little that the allocation of emissions from waste incineration are insignificant for the total emissions. In contrast, when there is no excess heat, the total emissions are very sensitive to how the emissions related to waste incineration are allocated, see Table S5.4 in Supplementary S5.7.3 for details.

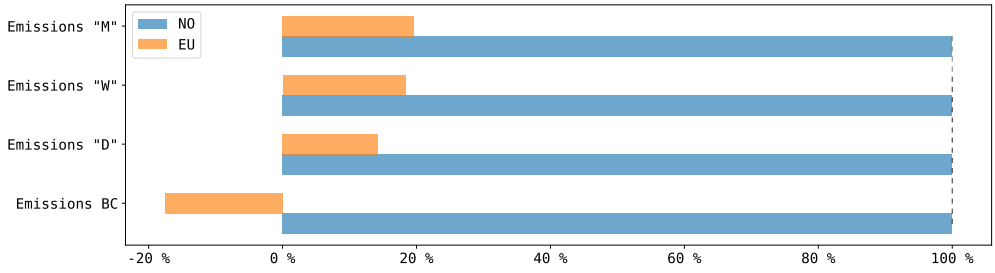

FIGURE 17 Sensitivity on average emissions measured in kg CO_2eq/m^2 and year with the EU28+NO scenario for emission intensity.

4 | DISCUSSION

This section discuss the input data, load matching strategy described in Section 2.3, and the results obtained in context with the research questions asked in 1.3. Results are elaborated on and compared to the literature assessed in the introduction.

4.1 | General Results

Achieving the climate change mitigation targets will require large energy savings and GHG emission reduction in the building stock and mobility sector. The development of ZEN concepts may facilitate these mitigation strategies. The stages of proposing, assessing and accepting ZEN design options, however, have to reflect many, sometimes conflicting, interests of the decision makers. In this comprehensive study, we develop a methodology that can be used in neighbourhood planning, based on a set of KPIs, and with Ravneberget as case study. We analyse how a finite set of likely combinations of EV charging can interact with load profiles and PV supply for the buildings in order to influence the energy and emission performance of the neighbourhood. It is also investigated how peak shaving and energy storage strategies affect this performance, including the interacting subsystems such as building energy demand, mobility needs, onsite energy generation, local energy storage, and import/export to external electricity grid. The emission calculations are performed by using the ZEN framework, focusing on operational emissions from energy supply and storage, mobility solutions and embodied emissions in onsite energy generation and storage technologies.

In general, different charging profiles for the shared EV pool result in various energy and emission performance, in this study measured by four KPIs. The results showed that when there was no peak shaving strategy, midday EV charging was desirable in terms of SC and SS. This confirms the findings in Denholm et al. [37]. Moreover, this solves the issue addressed by Munkhammar et al. [54] and Denholm et al. [37], of limited increase in SC when introducing EVs on aggregated building level due to the low coincidence between the PV power production and the charging pattern of the EVs. The storage components and grid exports also solve the issue outlined by Tummina et al. [61], where the utilisation of PV generation is poor, even if the production is high. Further, implementing storage components solves the issue of being obligated, and thus reliant, on using the PV power instantaneously as addressed in Denholm et al. [37].

The total operational emissions, i.e. building and mobility operation, accounts for 16.1% of the total emissions for base case, and reduces to 9%, 6.9% and 6.4% for the D, W and M peak shaving strategies respectively. Because of reduced exports of electricity (i.e. reduced negative emissions), and increased emissions from storage applications, the overall emissions increase. Hence, the operational emissions constitute a smaller share of the total, and the material emissions (mostly from PV panels) are dominating. The operational neighbourhood emissions are found much lower than the assessed literature [28, 72], finding these emissions to be responsible for 42-44% of the total neighbourhood emissions. Reasons for that are large emissions from storage, and a neighbourhood with electricity demand much lower than compared to other studies, due to the use of district heating and the shared EV pool covering the mobility service.

However, one could distribute the emissions embodied in PV panels to where the energy is actually consumed, i.e. either in building or mobility operation where the energy offsets import of electricity from the grid, or to exports, where emissions are compensated with a negative emission intensity. For base case, all onsite generation is either used in buildings or exported. As peak shaving is implemented, less energy is exported to the grid and more energy is consumed in charging of EVs. Hence, a larger share of the emissions can be allocated to mobility. When accounting for emissions from PV panels to where the PV energy is actually consumed, the total mobility operations are found

to be 12.5% for base case and 16.5%, 15.7% and 15.5% for D, W and M peak shaving strategy respectively. This confirms that as less PV energy is exported, a larger share of the emissions are allocated to mobility. The operational emissions from mobility in Lausselet et al. [28] are found to be 15%. However, this does not include the material emissions from PV panels, but does however contain direct emissions from fossil fuels. These findings underline the importance of emphasising that the material emissions in PV panels are significant, and even if EVs are fully supplied by onsite electricity for charging, they still have an environmental impact.

Because the neighbourhood heating and DHW demand is covered by district heating, rather small seasonal variations are to be found in the delivered electricity. As a result, there is little variation in charge/discharge curves among the different shaving strategies, especially between the weekly and monthly storage. In a neighbourhood consisting of all-electric buildings with large seasonal variations in electricity demand, a similar peak shaving strategy would probably mean that for longer time frames for peak shaving, larger storage capacities are required, so that energy in months with large onsite production (typically during the summer) can be stored and used in months with little onsite production (typically during the winter) [110]. This problem is solved if the heat demand is covered by district heating instead of electricity, especially when utilising excess heat, as in this case assumed with no environmental impacts. Literature also address the use of district heating to supply passive houses with high electricity demand to be a good alternative [111, 112]. The results also show that even after covering the heating demand in the neighbourhood, there were times where surplus heat were wasted, addressing the need for further investigating the potential of a thermal storage.

A combined day- and night charging profile was desirable in reducing maximum grid loads, and morning and afternoon charging (as from the questionnaire) was desirable in terms of lowering emissions. In order to investigate all aspects, here in terms of a selected number of KPIs, the optimal neighbourhood EV charging profile must be solved as a trade-off problem where the different KPIs needs to be valued, prioritised and/or specified with restrictions in order to fulfil the desired goals by DSM of EVs. The methodology developed in this study provides the opportunity of identifying which charging combinations are desired with criteria set as desired, The resulting energy and GHG emission performance of the neighbourhood can be illustrated by pair plotting the KPIs, as in Figure 13, pointing towards the desired and undesired charging combinations.

The pair plots shown in the results in order to interpret and visualise the relationships between the KPIs, can be useful as a MCDS tool in neighbourhood planning and operation. The pair plots illustrate that not only are the "Good" combinations satisfying the criteria set for each KPI, they are also providing a sufficient mobility service level. The results revealed that the charging combinations desired are composed by different charging profiles, meaning that the carpool will at all times have cars available for mobility service; as certain cars are charging in the morning and afternoon, and provide mobility service during midday, other cars are charging on midday, and provide mobility service in the morning and afternoon. This also solves the problem of all EVs in a shared car pool may lead to local grid overload if charging simultaneously [40]. Overall, the carpool solution assessed appears sufficient. In comparison of annual neighbourhood emissions, none of the assessed literature contain the same elements nor life cycle stages as in this study, and direct comparison is thus difficult.

4.2 | Sensitivity Analysis

The sensitivity analysis shows that as the total emissions are larger, the emissions are less sensitive to changes in certain parameters, as expected. This means that for charging combinations resulting in low total emissions, the relative importance of each parameter is larger than for charging combinations resulting in overall larger total emissions. Furthermore, the peak shaving strategies with longer time horizons are less sensitive to changes i parameters because

the total emissions are larger. However, if changes are made in components imposing these large emissions originally (e.g. batteries), changes in these parameters parameters affecting these components (e.g. travel length, number of charging cycles) impose a larger change than for strategies with lower emissions. This can be observed for M peak shaving strategy; when changing the travel length, emission intensity of storage and number of charging cycles, the total emissions changes significantly. The sensitivity also reveals that the SC is more sensitive to changes in parameters than the SS. This is because the PV production at Ravneberget is large, and so the neighbourhood is almost self-supplied when implementing peak shaving. Hence, if changing the electricity demand or the PV generation, the SS will not be very affected because the peak shaving algorithm is very efficient in reallocating the PV generated energy. However, the SC increase significantly because the peak shaving algorithm affect the amount of PV energy exported.

The assumption of an emission intensity of 0 g CO_2eq/kWh for the excess heat from the power transformer, is a critical assumption. Figure 2 illustrates that the energy demand for heat is 40.3% of the total delivered energy, but because of the large heat supply, the delivered district heat is only 0.8 ‰ of the heat that would be delivered without the excess heat available. Applying an emission intensity for delivered excess heat, for instance in terms of embodied emissions in building, operating and maintaining the transformer station, would have reflected more realistic results. Nevertheless, the sensitivity of having no excess heat from the transformer does confirm that the excess heat is a critical parameter for the total emission performance of the neighbourhood.

The importance of emission intensity of electricity is clearly depicted in Figure 17 and in Table S5.2 in Supplementary S5.7.1. Due to the assumption of symmetric weighting, the exported electricity with a European electricity mix is much higher than for the Norwegian, and as a result, the total neighbourhood emissions are lower. In fact, emissions can only be paid back if the PV systems emissions are lower than the emission factor in the grid. If negative emissions are disregarded, the total emissions would increase by 89% when changing from Norwegian to European electricity intensity, which emphasise this point. Lausselet et al. [15] finds this increase in total emissions to be 30%, however the total emissions in this study includes material emissions in buildings, mobility and infrastructure, accounting for 56% of the total emissions, and the relative increase in that study will thus be smaller. The point is that the symmetric weighting undermines the benefit of a low emission intensity of electricity, which is important to acknowledge. On the other hand, when exporting PV power, the grid electricity is substituted, which is beneficial if the emissions from PV generation is lower than the emission factor in the grid. Moreover, for countries like Norway having a low emission intensity of electricity, it will be even more important to export renewable energy as the power grid is getting connected to the European grid.

The sensitivity reveals that the total emissions are sensitive to the area of PV panels, confirming that lowering the embodied emissions in PV panels, as addressed in literature, is crucial in lowering the total neighbourhood emissions [20, 21]. The literature address the onsite generation system to constitute 5% of the total neighbourhood emissions after subtracting the compensated emissions from export [28], confirming that embodied emissions are significant. A direct comparison of material emissions to the literature is misleading due to the system boundaries of the emission assessment in this study. Further, the results revealed the importance of number of charging cycles, i.e. the battery lifetime, as outlined in the works of Ellingsen et al. [44]. The battery emissions increased the annual average emissions from base case with 24.1 - 32.1%, and increasing the lifetime of batteries would thus improve the emission performance of the neighbourhood significantly. The emissions from batteries are major drawbacks of the peak shaving strategies, especially since the other KPIs, max grid load, SC and SS, are improved when implementing peak shaving. Hence, this work should encourage the industry to strive to lower the emissions in Li-ion batteries, by increased efficiencies, efficient material use, the potential of reusing batteries etc. Furthermore, the most efficient way of reducing battery impacts are by lowering the emission intensity of electricity in the manufacturing stage [24, 44], illustrating the

importance of the emission intensity of electricity, not only in building and mobility operation but also in production of technical components and neighbourhood elements. Lastly, due to the various assumptions in LCAs of Li-ion batteries (e.g. number of charging cycles, DoDs, efficiencies etc.), conclusions on the environmental impacts of batteries are lying in the range of 38 to 338 kg CO_2eq./kWh [24], and therefore, there lies uncertainties to the assumption of 130.7 kg CO_2eq./kWh per installed capacity as used in this study. A standardisation of emission calculations of Li-ion batteries may provide robustness of impact calculations, which could be beneficial in neighbourhood planning.

As the emission intensity of electricity is a critical parameter, the evolution of electricity provides uncertainty to the calculations. Moreover, as addressed in Noussan and Neirotti [55], the impacts of EV charging with hourly profiles were found to be higher than those calculated with a mean for the emission factor, because of daily and seasonal variation in the electricity mix. Hence, the emissions calculated with average annual values in this study may be underestimated, and hourly emission factors could influence the decision of which charging combinations are beneficial. Further, Noussan and Neirotti [55] illustrate that when comparing morning, day and evening charging profiles, the morning charging has highest emissions, because under peak consumption, dispatchable fossil plants may be required to secure energy supply, increasing the hourly emission factor. Although they address that the variation in emissions when applying hourly emission factor are greater than the variations among the three different charging profiles themselves [55], the benefits of controlled charging may be more visible with hourly emission data. For instance, for a neighbourhood with no storage units, like base case, DSM could be used to restrict EV charging to times during the day when the emission intensity in the grid is low, typically during night. This might reduce the EV charging demand during daytime, and surplus PV generation could be exported, compensated with a higher emission intensity.

4.3 | Limitations and Further work

Due to the large scope of this study, there are limitations and uncertainties related to the methodology and results presented. First of all, the energy performance simulations are based on the assumption of all building units operating similar with input data fitting the NS3700 [1]. Accounting for various occupancy behaviour among the neighbourhood inhabitants and changes in behaviour over the assessed POA, would have provided more realistic results. The peak shaving algorithm relies heavily on data accuracy, and supplementing simulated data sets with measured data would be beneficial. Moreover, the PV generation is based on a weather file representing "typical" weather, and forecasts would provide more accuracy for the energy and GHG emission performance at Ravneberget. Furthermore, the mobility service level is assumed unchanged over the POA, which could contribute to overestimating the electricity consumption, if mobility service needs are in larger scale fulfilled by public transport and/or efficiencies improvements of EVs. The mobility service level relies heavily on the assumption of the neighbourhood being provided sufficient public transport facilities, hence the size of the shared EV pool is dimensioned accordingly. Whether or not the mobility service level is sufficient is therefore closely related to elements outside the system boundary. Although the results revealed charging combinations sufficient to fulfil mobility needs, the exact mobility service level when considering charging of the car pool is not investigated in depth. Regarding the energy storage, we did not account for the energy losses in the charging/discharging of batteries, as these are very technology specific, which could lead to underestimates of emissions from battery degradation.

Including material emissions in mobility (bodywork) and buildings, the embodied emissions in the power transformer, and infrastructure and networks, would provide a more holistic picture of the neighbourhood. Materials in infrastructure and networks in similar neighbourhood analysis are found to contribute with 2% of the total emissions [28], constituting a relatively small share of the total emissions. Further are materials from buildings and mobility

found to be accountable for 40% of the total emissions, with buildings constituting 52% of these, where 22% are embodied in materials and 31% are operational emissions. Lowering the operational emission in building operation is therefor significant, but less significant than for instance lowering the emissions in building envelopes. Moreover, as material emissions in neighbourhoods are found to be 55-87% of the total emissions [113], the emissions from batteries could be a relative small part of the total emissions. Hence, the drawback of the emission performance we present in this study could be less of a drawback in the bigger picture. Assessing several impact categories would have improved the robustness of the model. For example, a technology choice beneficial in a ZEN project in terms of GHG emissions may not be beneficial if considering impact categories such as acidification, land use changes etc. PV panels and Li-ion batteries are examples of technologies with drawbacks in these impact categories, and considering other impact categories may lead to different results. Further work may address the importance of these aspects and include the ones with highest significance and relevance.

The model does not consider long term changes in technology, besides the 50% emission reduction in the replacement of the PV panels. Efficiency improvements in the stationary and EV batteries and building envelopes, are factors adding uncertainties to the study. Especially for the critical parameters batteries and PV panels, one should consider that there are rapid changes, based on prior knowledge on the fast development of these technologies. There are also uncertainties related to the evolution of the electricity intensity and the process of which the Northern and European electricity grid will be fully connected. Another aspect is how investments in new technology and renewable energy sources may be threatened under the global Covid-19 crisis of early 2020, together with low oil prices. Nevertheless, could the crisis reveal the volatility and vulnerability of an economy strongly correlated to the oil price, thus accelerate the investments in research and development of mitigating technologies and renewable energy sources.

Overall, this work and the methodology developed contributes to a broader understanding of the interplay of onsite PV generation, electric vehicles sharing and battery storage for power peak shaving and can be useful in neighbourhood planning. Moreover, the results can come in handy in demand side management and decision making under operation of mobility. The results reveal which elements that contributes to the largest emissions, and how one must be careful in optimising only one energy performance indicator as this may come at the cost of reduced performance of others. Further work should consider expanding the system boundaries, accounting for embodied emissions in buildings, mobility and infrastructure, to better understand the interplay and trade-offs by controlling EV charging and implementing peak shaving. Investigating the possibilities of thermal storage, the use of retired batteries for EVs as stationary applications and the use of vehicle-to-grid technology, could enlighten other aspects than what addressed in this study, as well as adding complexity to the methodology developed. Assessing the effect of hourly emission intensities and how it may affect the selected KPIs, should be investigated. Further research may consider including aspects of technology improvements and changes in behaviour to increase the robustness and validity of the methodology and results. Lastly, the adaptive MCDS tool provided in this study, may be useful in neighbourhood planning and operation and should be considered for further development. This may include a larger number of KPIs to address several aspects of the neighbourhood's energy and GHG emission performance, such as grid influence, life cycle costs, etc.. which could reveal other desirable solutions for neighbourhood planning and management.

5 | CONCLUSION

In this paper, a comprehensive methodology was applied to the case neighbourhood Ravneberget, in order to investigate the emission and energy performance of a finite set of likely combinations of EV charging. It is also investigated how peak shaving and energy storage strategies affect this performance, including the interacting subsystems such

as building energy demand, mobility needs, onsite energy generation, local energy storage, and import/export to external electricity grid. The emission calculations are performed by using the ZEN framework, focusing on operational emissions from energy (supply and storage), mobility solutions and embodied emissions in onsite energy generation and storage technologies.

The results of this paper provide the estimates of how different charging combinations influence a set of energy and emission KPIs. The neighbourhood emissions increase with the implementation of peak shaving strategies. The more ambitious peak shaving strategy is - the larger are the associated emissions from battery degradation. Hence, there is a trade-off problem regarding energy and emission performance of the neighbourhood. Furthermore, the results reveals that the optimal (or the acceptable) charging combinations for the neighbourhood must be found by solving a multi-criteria problem, because the charging combinations having a good performance based on certain KPIs, not necessarily perform well based on the others. Hence, each of the combinations of EV charging were classified in different performance categories, here either "G", "M" or "P", based on which criteria that were satisfied for the KPIs. In adaptation of the methodology, stakeholders may change the KPIs and performance criteria, to fit their purpose.

Although the methodology developed can be useful in neighbourhood planning and DSM, the model is limited by simulated data, simplified battery models and uncertainties associated to several parameters, Further development of the peak shaving strategy, and the decision support tool provided in this study, is likely to make a significant contribution in neighbourhood planning and operation. However, further studies should consider other technical solutions and neighbourhood designs, as well as improve the aspects that are limiting the presented study. Especially for ZEN pilots, further development of this work is likely to provide energy flexibility of mobility service, buildings and neighbourhoods.

ACKNOWLEDGEMENTS

The authors gratefully acknowledge the support of the Research Council of Norway and several partners through the Research Centre on Zero Emission Neighbourhoods in Smart Cities (FME ZEN). This work was carried out as a part of a MSc. thesis at the Norwegian University of Science and Technology.

SUPPLEMENTARY MATERIALS

For this paper, it follows a supplement material, which describes the subsystems and methodology in detail, providing a broader understanding of the underlying assumptions and calculation procedures. The supplement material is referred to throughout the text.

References

[1] Standards Norway, "NS 3720 Method for greenhouse gas calculations for buildings," 2018.

[2] D. Giordano and F. Maiorana, "Teaching algorithms: Visual language vs flowchart vs textual language," *IEEE Global Engineering Education Conference, EDUCON*, vol. 2015-April, no. March, pp. 499–504, 2015.

[3] UN Environment and International Energy Agency, "2018 Global Status Report," p. 325, 2018.

[4] Thibaut Abergel, C. Delmastro, P. Janoska, K. Lane, and A. Prag, "Perspectives for the Clean Energy Transition," *IEA*, p. 117, 2019.

[5] D. Ürge-Vorsatz, O. Lucon, A. Zain Ahmed, H. Akbari, P. Bertoldi, L. F. Cabeza, N. Eyre, A. Gadgil, L. D. D Harvey, Y. Jiang, E. Liphoto, S. Mirasgedis, S. Murakami, J. Parikh, C. Pyke, and M. V. Vilariño, "Buildings. In: Mitigation. Working Group III contribution to the Fifth Assessment Report of the Intergovernmental Panel of Climate Change.," pp. 671–738, 2014.

[6] R. Banerjee, S. Benson, D. Bouille, A. Brew-Hammond, A. Cherp, S. Coelho, L. Emberson, M. Figueroa, A. Grubler, M. Jaccard, S. Ribeiro, S. Karekezi, K. He, E. Larson, Z. Li, S. McDade, L. Mytelka, S. Pachauri, A. Patwardhan, and T. Johansson, "Global Energy Assessment: Towards a Sustainable Future," *Management of Environmental Quality: An International Journal*, vol. 24, no. 3, pp. 98–102, 2013.

[7] R. Hickel, "Directive 2010/31/EU of the European Parliament and of the Coun- cil of 19 May 2010 on the energy performance of buildings (recast)," *Official Journal of the European Union*, vol. 63, no. 30, p. 619, 2010.

[8] IEA, "Global EV Outlook 2019," tech. rep., Paris, 2019.

[9] D. Fischer, A. Surmann, and K. B. Lindberg, "Impact of emerging technologies on the electricity load profile of residential areas," *Energy and Buildings*, vol. 208, p. 109614, 2 2020.

[10] P. Palensky and D. Dietrich, "Demand side management: Demand response, intelligent energy systems, and smart loads," *IEEE Transactions on Industrial Informatics*, vol. 7, no. 3, pp. 381–388, 2011.

[11] G. Strbac, "Demand side management: Benefits and challenges," *Energy Policy*, vol. 36, pp. 4419–4426, 12 2008.

[12] R. Luthander, J. Widén, D. Nilsson, and J. Palm, "Photovoltaic self-consumption in buildings: A review," *Applied Energy*, vol. 142, pp. 80–94, 3 2015.

[13] M. Lotteau, G. Yepez-Salmon, and N. Salmon, "Environmental Assessment of Sustainable Neighborhood Projects through NEST, a Decision Support Tool for Early Stage Urban Planning," *Procedia Engineering*, vol. 115, pp. 69–76, 1 2015.

[14] C. Skaar, N. Labonnote, and K. Gradeci, "From Zero Emission Buildings (ZEB) to Zero Emission Neighbourhoods (ZEN): A Mapping Review of Algorithm-Based LCA," 2018.

[15] C. Lausselet, L. A. W. Ellingsen, A. H. Strømman, and H. Brattebø, "A life-cycle assessment model for zero emission neighborhoods," *Journal of Industrial Ecology*, vol. 2020, pp. 1–17, 2019.

[16] M. Lotteau, P. Loubet, M. Pousse, E. Dufrasnes, and G. Sonnemann, "Critical review of life cycle assessment (LCA) for the built environment at the neighborhood scale," *Building and Environment*, vol. 93, pp. 165–178, 2015.

[17] RC on ZEB, "About the ZEB Centre," 2020.

[18] FME ZEN, "About Us – FME ZEN," 2020.

[19] Standards Norwegian, "ISO 14040:2006 Environmental management - Life cycle assessment - Re- quirements and guidelines," 2006.

[20] T. F. Kristjansdottir, C. S. Good, M. R. Inman, R. D. Schlanbusch, and I. Andresen, "Embodied greenhouse gas emissions from PV systems in Norwegian residential Zero Emission Pilot Buildings," *Solar Energy*, vol. 133, pp. 155–171, 2016.

[21] T. F. Kristjansdottir, A. Houlihan-Wiberg, I. Andresen, L. Georges, N. Heeren, C. S. Good, and H. Brattebø, "Is a net life cycle balance for energy and materials achievable for a zero emission single-family building in Norway?," *Energy and Buildings*, vol. 168, pp. 457–469, 2018.

[22] P. Chastas, T. Theodosiou, and D. Bikas, "Embodied energy in residential buildings-towards the nearly zero energy building: A literature review," *Building and Environment*, vol. 105, pp. 267–282, 2016.

[23] N. W. Brown, S. Olsson, and T. Malmqvist, "Embodied greenhouse gas emissions from refurbishment of residential building stock to achieve a 50% operational energy reduction," *Building and Environment*, vol. 79, pp. 46–56, 2014.

[24] L. Vandepaer, J. Cloutier, and B. Amor, "Environmental impacts of Lithium Metal Polymer and Lithium-ion stationary batteries," *Renewable and Sustainable Energy Reviews*, vol. 78, pp. 46–60, 10 2017.

[25] A. Opitz, P. Badami, L. Shen, K. Vignarooban, and A. Kannan, "Can Li-Ion batteries be the panacea for automotive applications?," *Renewable and Sustainable Energy Reviews*, vol. 68, pp. 685–692, 2 2017.

[26] J. F. Peters, M. Baumann, B. Zimmermann, J. Braun, and M. Weil, "The environmental impact of Li-Ion batteries and the role of key parameters – A review," *Renewable and Sustainable Energy Reviews*, vol. 67, pp. 491–506, 1 2017.

[27] P. Murray, K. Orehounig, D. Grosspietsch, and J. Carmeliet, "A comparison of storage systems in neighbourhood decentralized energy system applications from 2015 to 2050," *Applied Energy*, vol. 231, pp. 1285–1306, 12 2018.

[28] C. Lausselet, V. Borgnes, and H. Brattebø, "LCA modelling for Zero Emission Neighbourhoods in early stage planning," *Building and Environment*, vol. 149, no. October 2018, pp. 379–389, 2019.

[29] J. Oliver-Solà, A. Josa, A. P. Arena, X. Gabarrell, and J. Rieradevall, "The GWP-Chart: An environmental tool for guiding urban planning processes. Application to concrete sidewalks," *Cities*, vol. 28, pp. 245–250, 6 2011.

[30] A. Mastrucci, A. Marvuglia, U. Leopold, and E. Benetto, "Life Cycle Assessment of building stocks from urban to transnational scales: A review," *Renewable and Sustainable Energy Reviews*, vol. 74, pp. 316–332, 7 2017.

[31] B. G. Nichols and K. M. Kockelman, "Life-cycle energy implications of different residential settings: Recognizing buildings, travel, and public infrastructure," *Energy Policy*, vol. 68, pp. 232–242, 5 2014.

[32] J. Bastos, S. A. Batterman, and F. Freire, "Significance of mobility in the life-cycle assessment of buildings," *Building Research and Information*, vol. 44, no. 4, pp. 376–393, 2016.

[33] V. Nenseth, T. E. Julsrud, and M. Hald, "Nye kollektive bildeling som case," no. I, 2012.

[34] E. Martin, S. A. Shaheen, and J. Lidicker, "Impact of Carsharing on Household Vehicle Holdings: Results from North American Shared-Use Vehicle Survey," *Transportation Research Record*, vol. 2143, pp. 150–158, 1 2010.

[35] E. Martin and S. Shaheen, "Greenhouse gas emission impacts of carsharing in North America," *IEEE Transactions on Intelligent Transportation Systems*, vol. 12, no. 4, pp. 1074–1086, 2011.

[36] S. A. Shaheen and A. P. Cohen, "Carsharing and Personal Vehicle Services: Worldwide Market Developments and Emerging Trends," *International Journal of Sustainable Transportation*, vol. 7, pp. 5–34, 1 2013.

[37] P. Denholm, M. Kuss, and R. M. Margolis, "Co-benefits of large scale plug-in hybrid electric vehicle and solar PV deployment," *Journal of Power Sources*, vol. 236, pp. 350–356, 8 2013.

[38] H. Estes, S. Santoso, and G. Fisher, "Analysis of high-resolution electric vehicle charging on time-of-use grid demands," in *2015 IEEE Power & Energy Society General Meeting*, pp. 1–5, 2015.

[39] C. H. Skotland, E. Eggum, and D. Spilde, *Hva betyr elbiler for strømnettet?* NVE, 2016.

[40] I. Momber, T. Gómez, G. Venkataramanan, M. Stadler, S. Beer, J. Lai, C. Marnay, and V. Battaglia, "Plug-in electric vehicle interactions with a small office building: An economic analysis using DER-CAM," in *IEEE PES General Meeting, PES 2010*, 2010.

[41] NVE, "Hvordan vil en omfattende elektrifisering av transportsektoren påvirke kraftsystemet?," tech. rep., NVE, 2016.

[42] L. Sørensen, S. Jiang, B. N. Torsæter, and S. Völler, "Smart EV charging systems for zero emission neighbourhoods," Tech. Rep. 5, SINTEF Building Infrastructure, 2018.

[43] D. Fischer, A. Harbrecht, A. Surmann, and R. McKenna, "Electric vehicles' impacts on residential electric local profiles – A stochastic modelling approach considering socio-economic, behavioural and spatial factors," *Applied Energy*, vol. 233-234, pp. 644–658, 1 2019.

[44] L. A. W. Ellingsen, G. Majeau-Bettez, B. Singh, A. K. Srivastava, L. O. Valøen, and A. H. Strømman, "Life Cycle Assessment of a Lithium-Ion Battery Vehicle Pack," *Journal of Industrial Ecology*, vol. 18, no. 1, pp. 113–124, 2014.

[45] G. Majeau-Bettez, T. Hawkins, and A. Strømman, "Life Cycle Environmental Assessment of Lithium-Ion and Nickel Metal Hydride Batteries for Plug-In Hybrid and Battery Electric Vehicles," *Environmental science & technology*, vol. 45, p. 5454, 6 2011.

[46] J. B. Dunn, L. Gaines, J. C. Kelly, C. James, and K. G. Gallagher, "The significance of Li-ion batteries in electric vehicle life-cycle energy and emissions and recycling's role in its reduction," *Energy and Environmental Science*, vol. 8, pp. 158–168, 12 2015.

[47] H. C. Kim, T. J. Wallington, R. Arsenault, C. Bae, S. Ahn, and J. Lee, "Cradle-to-Gate Emissions from a Commercial Electric Vehicle Li-Ion Battery: A Comparative Analysis," *Environmental Science and Technology*, vol. 50, no. 14, pp. 7715–7722, 2016.

[48] E. Blasius and Z. Wang, "Effects of charging battery electric vehicles on local grid regarding standardized load profile in administration sector," *Applied Energy*, vol. 224, pp. 330–339, 8 2018.

[49] H. Mehrjerdi and E. Rakhshani, "Vehicle-to-grid technology for cost reduction and uncertainty management integrated with solar power," *Journal of Cleaner Production*, vol. 229, pp. 463–469, 8 2019.

[50] I. Cvetkovic, T. Thacker, D. Dong, G. Francis, V. Podosinov, D. Boroyevich, F. Wang, R. Burgos, G. Skutt, and J. Lesko, "Future home uninterruptible renewable energy system with vehicle-to-grid technology," in *2009 IEEE Energy Conversion Congress and Exposition, ECCE 2009*, pp. 2675–2681, 2009.

[51] H. Turton and F. Moura, "Vehicle-to-grid systems for sustainable development: An integrated energy analysis," *Technological Forecasting and Social Change*, vol. 75, pp. 1091–1108, 10 2008.

[52] C. Battistelli, L. Baringo, and A. Conejo, "Optimal energy management of small electric energy systems including V2G facilities and renewable energy sources," *Electric Power Systems Research*, vol. 92, pp. 50–59, 11 2012.

[53] H. Yang, T. Xiong, J. Qiu, D. Qiu, and Z. Y. Dong, "Optimal operation of DES/CCHP based regional multi-energy prosumer with demand response," *Applied Energy*, vol. 167, pp. 353–365, 4 2016.

[54] J. Munkhammar, P. Grahn, and J. Widén, "Quantifying self-consumption of on-site photovoltaic power generation in households with electric vehicle home charging," *Solar Energy*, vol. 97, pp. 208–216, 11 2013.

[55] M. Noussan, "Cross-Country Comparison of Hourly Electricity Mixes for EV Charging Profiles," pp. 1–14, 2020.

[56] E. Figenbaum and M. Kolbenstvedt, *Learning from Norwegian Battery Electric and Plug-in Hybrid Vehicle Users*. 2016.

[57] H. Thorgersen, T. Supervisor, . Patrick, and A. Narbel, "Large scale transition from conventional to electric vehicles and the consequences for the security of electricity supply A demand side analysis of electricity consumption NORWEGIAN SCHOOL OF ECONOMICS," tech. rep.

[58] L. Zhang, T. Brown, and G. S. Samuelsen, "Fuel reduction and electricity consumption impact of different charging scenarios for plug-in hybrid electric vehicles," *Journal of Power Sources*, vol. 196, pp. 6559–6566, 8 2011.

[59] P. Denholm and W. Short, "An Evaluation of Utility System Impacts and Benefits of Optimally Dispatched Plug-In Hybrid Electric Vehicles," *NREL Report noTP-620*, no. October, p. 41, 2006.

[60] M. Kintner-Meyer, K. Schneider, and R. Pratt, "Impacts assessment of plug-in hybrid vehicles on electric utilities and regional US power grids part 1: Technical analysis," *Pacific Northwest National Laboratory*, no. December 2007, pp. 1–18, 2007.

[61] G. Tumminia, F. Guarino, S. Longo, D. Aloisio, S. Cellura, F. Sergi, G. Brunaccini, V. Antonucci, and M. Ferraro, "Grid interaction and environmental impact of a net zero energy building," *Energy Conversion and Management*, vol. 203, p. 112228, 1 2020.

[62] M. H. J. Bollen, Y. Yang, and F. Hassan, "Integration of distributed generation in the power system - a power quality approach," in *2008 13th International Conference on Harmonics and Quality of Power*, pp. 1–8, 2008.

[63] P. Grahn, J. Munkhammar, J. Widén, K. Alvehag, and L. Söder, "PHEV Home-Charging Model Based on Residential Activity Patterns," *IEEE Transactions on Power Systems*, vol. 28, no. 3, pp. 2507–2515, 2013.

[64] J. Munkhammar, J. Widén, P. Grahn, and J. Rydén, "A Bernoulli distribution model for plug-in electric vehicle charging based on time-use data for driving patterns," in *2014 IEEE International Electric Vehicle Conference (IEVC)*, pp. 1–7, 2014.

[65] P. Denholm and R. M. Margolis, "Evaluating the limits of solar photovoltaics (PV) in electric power systems utilizing energy storage and other enabling technologies," *Energy Policy*, vol. 35, pp. 4424–4433, 9 2007.

[66] J. Salom, J. Widén, J. Candanedo, I. Sartori, K. Voss, and A. Marszal, "Understanding net zero energy buildings: Evaluation of load matching and grid interaction indicators," *Proceedings of Building Simulation 2011: 12th Conference of International Building Performance Simulation Association*, no. November, pp. 2514–2521, 2011.

[67] D. Yang, C. Lu, and G. Qi, "An Improved Electric Model with Online Parameters Correction for Large Li-Ion Battery Packs," *International Journal of Computer and Electrical Engineering*, vol. 5, no. 3, pp. 330–333, 2013.

[68] J. Zhao, S. Kucuksari, E. Mazhari, and Y.-J. Son, "Integrated analysis of high-penetration PV and PHEV with energy storage and demand response," *Applied Energy*, vol. 112, pp. 35–51, 2013.

[69] X. Wu, X. Hu, Y. Teng, S. Qian, and R. Cheng, "Optimal integration of a hybrid solar-battery power source into smart home nanogrid with plug-in electric vehicle," *Journal of Power Sources*, vol. 363, pp. 277–283, 2017.

[70] O. Erdinc, N. G. Paterakis, T. D. P. Mendes, A. G. Bakirtzis, and J. P. S. Catalão, "Smart Household Operation Considering Bi-Directional EV and ESS Utilization by Real-Time Pricing-Based DR," *IEEE Transactions on Smart Grid*, vol. 6, no. 3, pp. 1281–1291, 2015.

[71] Y.-H. Chiang, W.-Y. Sean, C.-H. Wu, and C.-Y. Huang, "Development of a converterless energy management system for reusing automotive lithium-ion battery applied in smart-grid balancing," *Journal of Cleaner Production*, vol. 156, pp. 750–756, 2017.

[72] A. Stephan, B. Battke, M. D. Beuse, J. H. Clausdeinken, and T. S. Schmidt, "Limiting the public cost of stationary battery deployment by combining applications," *Nature Energy*, vol. 1, no. 7, pp. 1–9, 2016.

[73] Q. Dai, J. C. Kelly, L. Gaines, and M. Wang, "Life cycle analysis of lithium-ion batteries for automotive applications," *Batteries*, vol. 5, no. 2, 2019.

[74] D. Gudmunds, E. Nyholm, M. Taljegard, and M. Odenberger, "Self-consumption and self-sufficiency for household solar producers when introducing an electric vehicle," *Renewable Energy*, vol. 148, pp. 1200–1215, 4 2020.

[75] B. D. Olaszi and J. Ladanyi, "Comparison of different discharge strategies of grid-connected residential PV systems with energy storage in perspective of optimal battery energy storage system sizing," 2017.

[76] F. Putois, "Market for nickel-cadmium batteries," *Journal of Power Sources*, 1995.

[77] P. Marques, R. Garcia, L. Kulay, and F. Freire, "Comparative life cycle assessment of lithium-ion batteries for electric vehicles addressing capacity fade," *Journal of Cleaner Production*, 2019.

[78] J. Wang, P. Liu, J. Hicks-Garner, E. Sherman, S. Soukiazian, M. Verbrugge, H. Tataria, J. Musser, and P. Finamore, "Cycle-life model for graphite-LiFePO4 cells," *Journal of Power Sources*, 2011.

[79] H. He, R. Xiong, and H. Guo, "Online estimation of model parameters and state-of-charge of LiFePO4 batteries in electric vehicles," *Applied Energy*, 2012.

[80] D. A. Notter, M. Gauch, R. Widmer, P. Wäger, A. Stamp, R. Zah, and H. J. Althaus, "Contribution of Li-ion batteries to the environmental impact of electric vehicles," *Environmental Science and Technology*, 2010.

[81] F. Freire and P. Marques, "Electric vehicles in Portugal: An integrated energy, greenhouse gas and cost life-cycle analysis," in *IEEE International Symposium on Sustainable Systems and Technology*, 2012.

[82] J. Garcia, D. Millet, P. Tonnelier, S. Richet, and R. Chenouard, "A novel approach for global environmental performance evaluation of electric batteries for hybrid vehicles," *Journal of Cleaner Production*, 2017.

[83] R. Frischknecht and K. Flury, "Life cycle assessment of electric mobility: Answers and challenges-Zurich, April 6, 2011," *International Journal of Life Cycle Assessment*, 2011.

[84] T. R. Hawkins, B. Singh, G. Majeau-Bettez, and A. H. Strømman, "Comparative Environmental Life Cycle Assessment of Conventional and Electric Vehicles," *Journal of Industrial Ecology*, 2013.

[85] Y. Ma, R. Y. Ke, R. Han, and B. J. Tang, "The analysis of the battery electric vehicle's potentiality of environmental effect: A case study of Beijing from 2016 to 2020," *Journal of Cleaner Production*, 2017.

[86] C. Samaras and K. Meisterling, "Life cycle assessment of greenhouse gas emissions from plug-in hybrid vehicles: Implications for policy," *Environmental Science and Technology*, 2008.

[87] R. Faria, P. Marques, P. Moura, F. Freire, J. Delgado, and A. T. de Almeida, "Impact of the electricity mix and use profile in the life-cycle assessment of electric vehicles," *Renewable and Sustainable Energy Reviews*, vol. 24, pp. 271–287, 8 2013.

[88] J. Vetter, P. Novák, M. R. Wagner, C. Veit, K. C. Möller, J. O. Besenhard, M. Winter, M. Wohlfahrt-Mehrens, C. Vogler, and A. Hammouche, "Ageing mechanisms in lithium-ion batteries," *Journal of Power Sources*, 2005.

[89] X. Han, L. Lu, Y. Zheng, X. Feng, Z. Li, J. Li, and M. Ouyang, "A review on the key issues of the lithium ion battery degradation among the whole life cycle," *eTransportation*, 2019.

[90] S. Jenu, I. Deviatkin, A. Hentunen, M. Myllysilta, S. Viik, and M. Pihlatie, "Reducing the climate change impacts of lithium-ion batteries by their cautious management through integration of stress factors and life cycle assessment," *Journal of Energy Storage*, vol. 27, p. 101023, 2020.

[91] J. Liu, Q. Duan, M. Ma, C. Zhao, J. Sun, and Q. Wang, "Aging mechanisms and thermal stability of aged commercial 18650 lithium ion battery induced by slight overcharging cycling," *Journal of Power Sources*, 2020.

[92] N. Heeren, C. L. Mutel, B. Steubing, Y. Ostermeyer, H. Wallbaum, and S. Hellweg, "Environmental Impact of Buildings—What Matters?," *Environmental Science & Technology*, vol. 49, pp. 9832–9841, 7 2015.

[93] O. Dahlstrøm, K. Sørnes, S. T. Eriksen, and E. G. Hertwich, "Life cycle assessment of a single-family residence built to either conventional- or passive house standard," *Energy and Buildings*, vol. 54, pp. 470–479, 11 2012.

[94] T. H. Dokka and K. Hellad, "med passivhusstandard Disposisjon," pp. 1–30.

[95] F. Selamawit, R. Schlanbudch, K. Sørnes, M. Inman, and I. Andresen, "A Norwegian ZEB Definition Guideline," Tech. Rep. January, SINTEF Academic Press Selamawit, 1 2016.

[96] Z. Wu, M. Wang, J. Zheng, X. Sun, M. Zhao, and X. Wang, "Life cycle greenhouse gas emission reduction potential of battery electric vehicle," *Journal of Cleaner Production*, vol. 190, pp. 462–470, 7 2018.

[97] I. Sartori, A. Napolitano, and K. Voss, "Net zero energy buildings: A consistent definition framework," *Energy and Buildings*, vol. 48, pp. 220–232, 5 2012.

[98] Sweco, "Ravneberget," 2019.

[99] M. E. Ingebretsen, "Muligheter for konvertering av eksisterende bygninger til lavtemperatur fjernvarme," 2014.

[100] Standards Norway, "NS 3700 Criteria for Passive Houses and Low Energy and Passive Standard," *Standard Norway*, 2013.

[101] EQUA, "Climate data download centre."

[102] SSB, "Befolkningen," 2019.

[103] SSB, "Bilparken," 2019.

[104] SSB, "Kjørelengder," 2019.

[105] R. Carlson, H. Lohse-Busch, J. Diez, and J. Gibbs, "The Measured Impact of Vehicle Mass on Road Load Forces and Energy Consumption for a BEV, HEV, and ICE Vehicle," *SAE International Journal of Alternative Powertrains*, vol. 2, pp. 105–114, 5 2013.

[106] M. Aunedi, M. Woolf, M. Bilton, G. Strbac, M. Aunedi, M. Woolf, M. Bilton, and G. Strbac, "Impact and opportunities for wide-scale EV deployment: Low Carbon London Learning Lab," no. October, 2014.

[107] R. P. Stanley, *Enumerative Combinatorics*, vol. 1. Cambridge: Cambridge University Press, 1997.

[108] Fjernkontrollen.no, "BKK Varme," 2018.

[109] V. M. Fthenakis, R. Frischknecht, M. Raugei, H. C. Kim, E. Alsema, M. Held, and M. de Wild Scholten, "Methodology Guidelines on Life Cycle Assessment of Photovoltaic Electricity," *Methodology Guidelines on Life Cycle Assessment of Photovoltaic Electricity*, vol. IEA PVPS T, no. 5454, p. International Energy Agency Photovoltaic Power Sys, 2011.

[110] R. Zhuravchak, N. Nord, and H. Brattebø, "Control strategy for battery-supported photovoltaic systems aimed at peak load reduction," *E3S Web of Conferences*, vol. 111, no. 201 9, 2019.

[111] B. Brunklaus, C. Thormark, and H. Baumann, "Illustrating limitations of energy studies of buildings with LCA and actor analysis," *Building Research & Information*, vol. 38, pp. 265–279, 6 2010.

[112] A. Dodoo, L. Gustavsson, and R. Sathre, "Building energy-efficiency standards in a life cycle primary energy perspective," *Energy and Buildings*, vol. 43, pp. 1589–1597, 7 2011.

[113] M. K. Wiik, S. M. Fufa, T. Kristjansdottir, and I. Andresen, "Lessons learnt from embodied GHG emission calculations in zero emission buildings (ZEBs) from the Norwegian ZEB research centre," *Energy and Buildings*, vol. 165, pp. 25–34, 2018.

[114] NTNU and SINTEF, *ENØK i Bygninger*. Gyldendal undervisning, 3 ed., 2007.

[115] Standards Norway, "SN-NSPEK 3031 Energy performance of buildings," 2020.

[116] A. Baggini, "Power Transformers – Introduction to measurement of losses," no. August, 2016.

[117] Siemens AG, "Transformers," *Siemens Power Engineering Guide*, p. 21, 2010.

[118] R. Turconi, A. Boldrin, and T. Astrup, "Life cycle assessment (LCA) of electricity generation technologies: Overview, comparability and limitations," *Renewable and Sustainable Energy Reviews*, vol. 28, pp. 555–565, 12 2013.

[119] T. L. Warranty, "SunPower Limited Product and Power Warranty for PV Modules," vol. 1, 2012.

[120] M. Horne, "District Heating BKK," 2020.

[121] M. Løseth, "Klimaregnskap for fjernvarme," *Norsk Energi*, 2014.

Supplementary Material

This document is supplementary material to the paper *Energy and GHG Emission Performance Profiles at Ravneberget in Bergen – The Interplay of Onsite PV Generation, Electric Vehicles Sharing and Battery Storage for Power Peak Shaving.* It describes the subsystems and methodology in detail, providing a broader understanding of the underlying assumptions and calculation procedures.

S1 | NEIGHBOURHOOD

The Ravneberget neighbourhood is in early planning stage and only the conceptual proposal design has been published. Some parameters are designed to fit the project plan, others are assumed and determined due to lack of data and/or for simplicity. Figure S1.1 is retrieved from the conceptual design proposal [98].

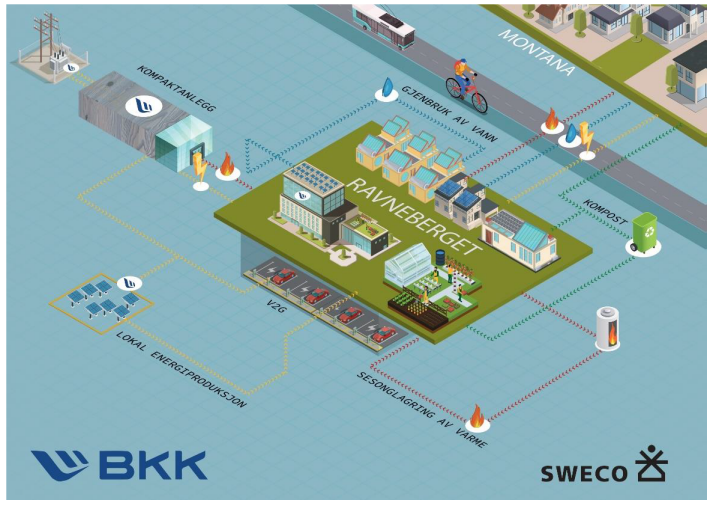

FIGURE S1.1 Sketch from the conceptual design proposal.

S1.1 | Building specific

The simulated unit is a two stories apartment of 130 m^2, see Figure S1.2 below. There are 45 m^2 with PV panels and 6.5 m^2 of solar collectors on each unit, each energy system mounted as one large panel for simplicity. Each unit is divided into seven zones; three bedrooms, two bathrooms, kitchen/living room and an entry, as shown in the floor plan in Figure S1.3. In line with the standard for passive houses and low energy buildings NS3700 [100], the window area is 15% of the gross floor area (GFA).

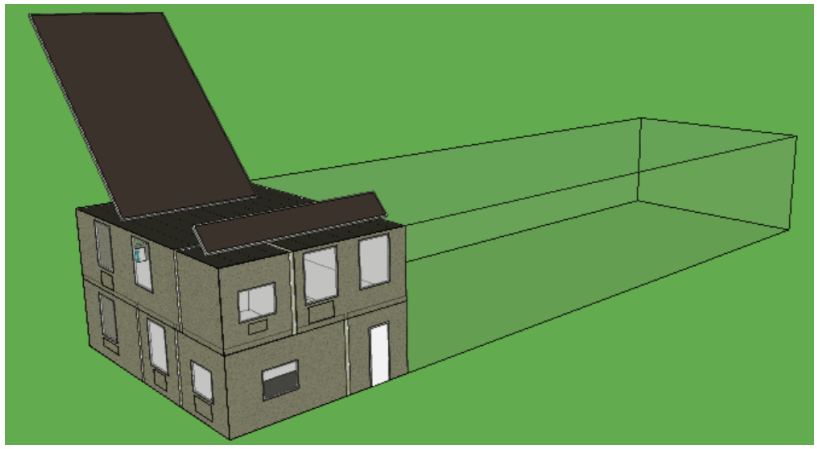

FIGURE S1.2 3D illustration of demo building simulated in IDA ICE. In order to assess the critical case, the end apartment in a vertical split is the chosen demo building.

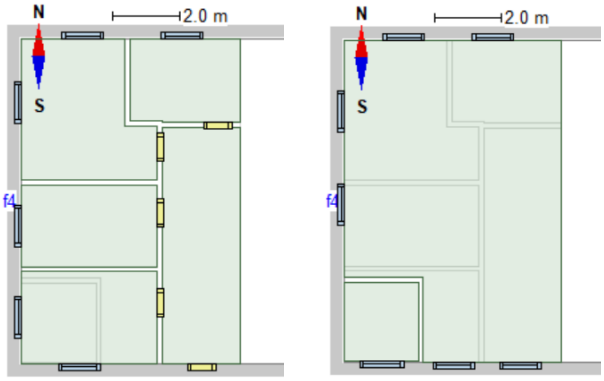

FIGURE S1.3 Floor plan of demo building: first floor to the left, second floor to the right.

S1.1.1 | Household electricity

In order to simulate a realistic housing unit, internal loads from equipment, lighting and excess heat are included in the model. The model is based on "ENØK i Bygninger" [114] and the standards for annual electricity requirement for low energy buildings and passive houses [100]. Annual delivered electricity for equipment and lighting are 18.1 and 6.8 kWh/m^2 respectively. Equipment and lighting are installed in each of the zones. The implemented ventilation system is a balanced mechanical constant Air Volume (CAV) system, with flow rates of 0.33 L/sm^2. Figure S1.4 shows the total electricity demand given in kWh/m^2 and year, for the building units and mobility service, and onsite PV generation.

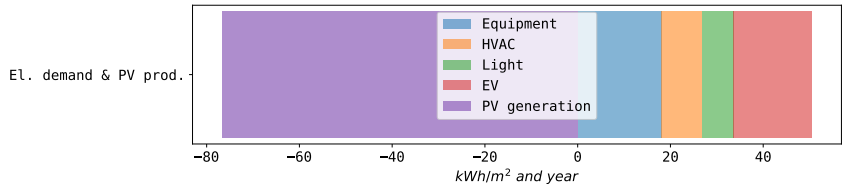

FIGURE S1.4 PV generation and the electrical energy use per building unit, including the EV charging.

The PV panels are mounted on a flat roof, south orientated with a 45° tilt and with an efficiency of 30%. The PV output is calculated based on real time weather data from the ASHRAE database [101], here for Bergen, Paradis. The peak power of 13.18 kW per building unit the generated PV output is calculated by:

$$P_{PV}(t) = \eta \cdot A \cdot I \cdot G(t) \tag{S1.0}$$

$P_{PV}(t)$ is the power output over time, η is the efficiency of the PV system, A is the PV area (m^2), and G(t) is the incident solar radiation (W/m^2). Table S1.1 shows the annual PV production for the neighbourhood.

TABLE S1.1 Neighbourhood PV output.

kWh/m^2 floor area and year	MWh/year	MWh/POA
76.0	1208.3	72499.4

S1.1.2 | Household heating

Highly energy efficient buildings with low demand for heating are usually constructed with a low temperature system. In this study the operating supply and return temperatures are 60°C and 40°C at a desired air temperature of 20°C. The choice of radiators and their location are described in the MSc thesis of Ingebretsen [99]. Figure S1.5 shows delivered heat to space heating and domestic hot water (DHW), collected heat from solar collectors, both with and without excess heat from the transformer.

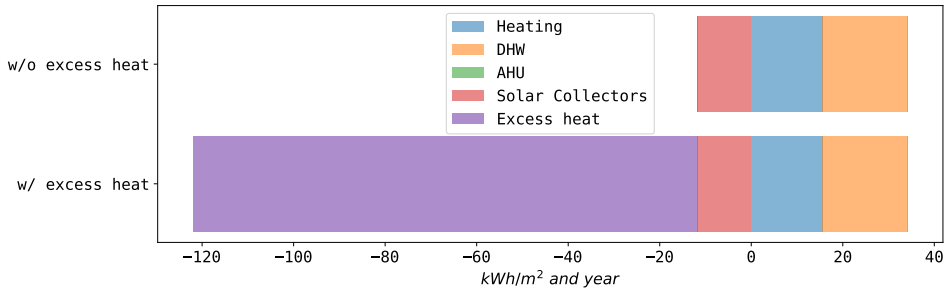

FIGURE S1.5 The heat specific demand with (to the left) and without (to the right) supply of excess heat from transformer station.

The neighbourhood is to be located within the concession area of district heating and is therefore modelled with district heating. The DHW requirements are 29.8 kWh/m^2 based on the specification SN-NSPEK 3031 [115]. The 6.4 m^2 solar collectors, dimensioned with similar collector area/GFA ratio as in the conceptual ZEBs in [21], collects 11.35 kWh/m^2 annually. Additionally, the excess heat from the transformer station, which will be compressed and rehabilitated for the Ravneberget project, will supply the neighbourhood with a constant heat of 200 kW. These are core losses from the transformer, further elaborated in S1.1.3. Figure S1.6 illustrates the plant model of the demo building unit as it is defined in IDA ICE.

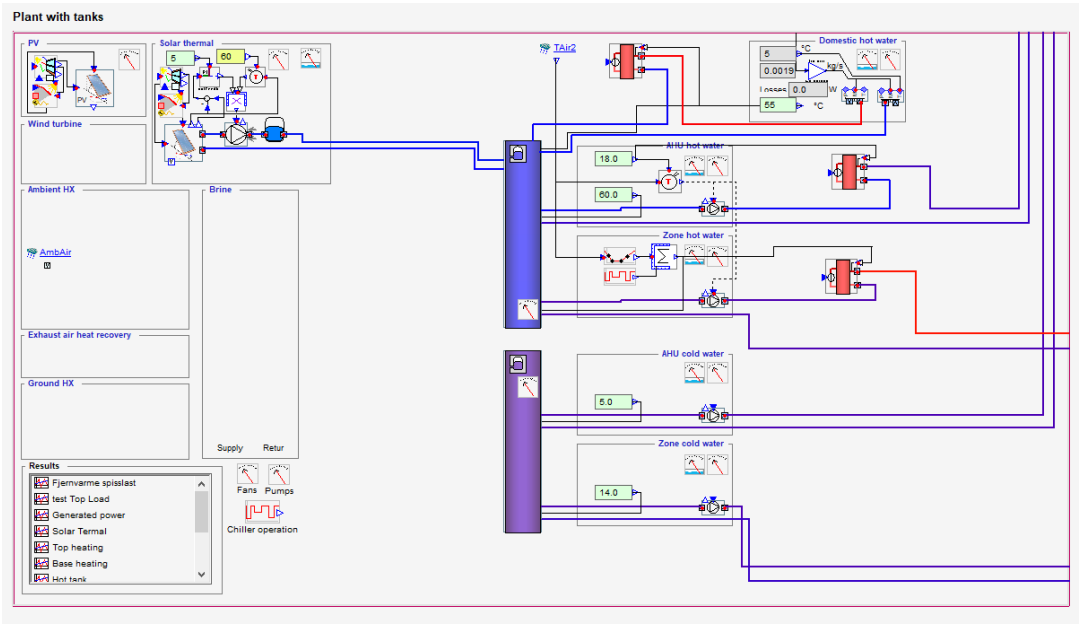

FIGURE S1.6 Plant model from IDA ICE of the ZEB demo.

S1.1.3 | Transformer losses

As BKK Nett AS are reconstructing and compressing the excising transformer station at Montana, Bergen, the remaining area is wished to be used in line with the Municipal business plan, with intention of giving something valuable back to the society. Exploitation of the excess heat, i.e. heat losses, from the transformer station in the neighbourhood buildings is therefore desired.

Losses in a transformer can be divided in two types of losses: no-load losses and load losses. The load losses, often called copper losses, are dependent on the loading pattern of the transformer. These losses are composed by the copper losses (also called RI^2 losses) and the conductor Eddy current losses. Due to lack of data, this study disregard the load losses and will only consider no-load losses. No-load losses occurs in the core of the transformer, regardless of whether there is any load or not. The no-load losses are composed by the hysteresis losses, Eddy current losses and dielectric losses. The latter usually accounts for less than 1% of the total no-load losses, whereas the former two account for 50% to 80% and 20% to 50% respectively. Hysteresis losses are "*caused by a frictional movement of magnetic domains in the core laminations being magnetised and demagnetised by alternation of the magnetic field*" [116], and will vary with the core material. The eddy-current losses are "*caused by varying magnetic fields inducing eddy currents in the laminations and thus generating heat*" [116].

In the case neighbourhood, four new transformers, each of 25/31.5 MVA, estimated to dissipate 200 to 450 kW of heat (depending on the load) are planned. In this study it is assumed that the lower bound value are the no-load losses, which will be utilised in the neighbourhood. I.e. it is assumed a constant heat supply of 200 kW to the neighbourhood, and all further losses are disregarded. For a 20/31.5 MVA power transformer, the no-load losses are constituting 12.75% of the total losses, according to Siemens Power Engineering Guide [117]. Utilising the no-load losses is therefor significant, but further research should strive to also include load losses. Figure S1.7 illustrates delivered heat from district heat with and without the continuous heat supplied by the transformer.

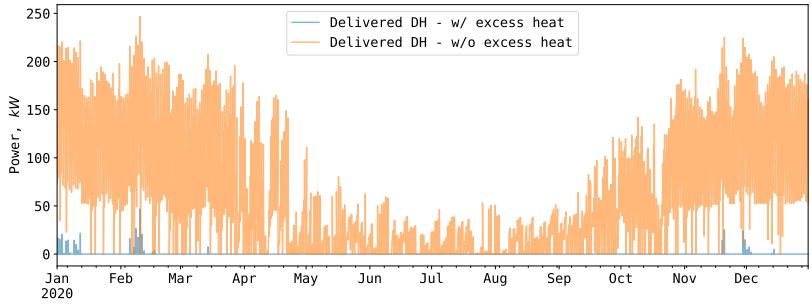

FIGURE S1.7 Delivered heat to the neighbourhood with and without excess heat supply from the transformer station.

S2 | MOBILITY

The mobility service level is calculated below. Table S2.1 provides the statistics needed in the calculations of dimensioning the shared car pool and is based on Statistics Norway [102, 103, 104]. It is assumed that one shared vehicle substitute five private vehicles and that the distance driven per person in a shared car pool is reduced by one third [33].

TABLE S2.1 Data for mobility calculations based on SSB.

Travel length km/year	Cars per person	Car substitution factor	Energy intensity
11 145	0.5229	1 shared : 5 private	0.2 kWh/km

The total number of cars in the neighbourhood:

$$\begin{aligned} \text{Number of cars} &= 0.5229 \frac{car}{person} \cdot 2.6 \frac{pers}{unit} \cdot 130 \frac{units}{neighbourhood} \cdot \frac{1}{5} \frac{car_{pool}}{car_{priv}} \\ &\approx 36 \end{aligned} \tag{S2.1}$$

Total distance driven in neighbourhood:

$$\begin{aligned} \text{Annual km per neighbourhood} &= 36 \cdot 11145 \frac{km}{car} \cdot 5 \frac{km\,car_{pool}}{km\,car_{priv}} \cdot \frac{2}{3} \frac{km_{car pool}}{km_{no\,car pool}} \\ &= 1337400 \\ \text{Annual km per car} &= 37150 \end{aligned} \tag{S2.1}$$

Energy consumption per car:

$$\begin{aligned} \text{Annual energy consumption} &= 37150 \frac{km}{car\ and\ year} \cdot 0.2 \frac{kWh}{km} = 7430 \frac{kWh}{car\ and\ year} \\ \text{Daily energy consumption} &= 20.4 \frac{kWh}{car\ and\ day} \end{aligned} \tag{S2.1}$$

S2.1 | Charging profiles

The data is generated with the use of mean charging values and standard deviations, and a probability distribution for charging at a given time in order to match load profiles retrieved from a questionnaire among EV owners [57]. The final mobility from IDA ICE results in 20.5 kWh/day and car, and not 20.4 kWh/day and car as calculated above. This is due to the simulated profiles in Excel, used as input in IDA ICE are based on a probability distribution for charging profile 1, in order to obtain the same curve as in the questionnaire [57]. The 0.1 kWh/day error increases the daily driving distance by 0.8 km per car, thus affects the mobility service level marginally. The input data is therefor set to 20.5 kWh/day in this study. Figure S2.1 and Figure S2.2 illustrate the neighbourhood energy load, heat supply and PV generation for a week in February when all EVs charge with profile 2 and 3 respectively.

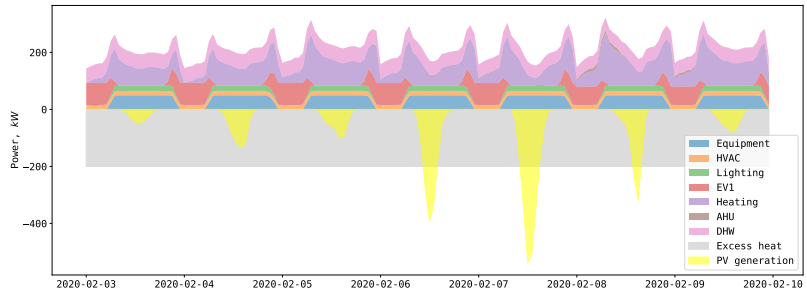

FIGURE S2.1 Neighbourhood energy load, heat supply and PV generation for a week in February, when all EVs charge with profile EV2.

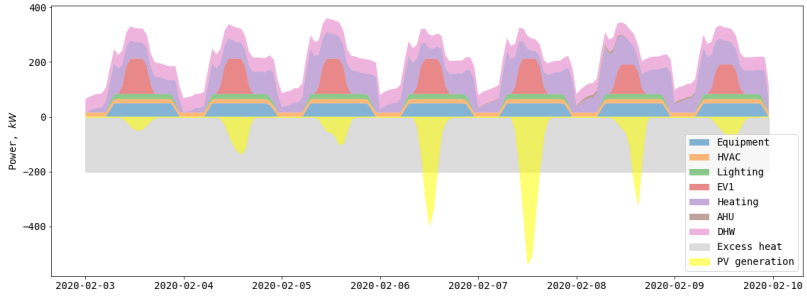

FIGURE S2.2 Neighbourhood energy load, heat supply and PV generation for a week in February, when all EVs charge with profile EV3.

S2.2 | Summary

Table S2.2 summarises the electricity and heating requirement for the building compared to NS 3700 stating the required prerequisites for passive houses and low energy buildings in Norway, in addition to the energy demand for mobility per car and per square meter.

TABLE S2.2 Energy use and heating demand for the building type.

	Electricity specific kWh/m^2			**Heat specific** kWh/m^2			**Mobility** kWh/m^2 (kWh/car and day)
	El. equipment	HVAC aux.	Lighting	Heating	AHU	DHW	EV eq.
Zeb Demo	18.1	8.64	6.83	15.64	0.09	18.36	15.95 (20.5)
NS 3700	17.5	9.0	7.0	16.0	0.0	18.0	-

S3 | EMISSION INTENSITIES

S3.1 | Electricity

The Norwegian Standard on method for greenhouse gas calculations in buildings [1] suggests two scenarios for evolution of the emission intensity: the Norwegian (NO) and European (EU28+NO) production mix. Each of the scenarios take today's production mix as a reference, and assumes as linear decrease based on Turconi et. al [118] to predict the evolution of the mix. The evolution of the electricity mix are found for a Norwegian electricity grid isolated from all import/export of electricity, and a European electricity mix, with import and export among the European countries including Norway. See Table S3.1 for details on emission intensity calculations.

TABLE S3.1 Calculated production mix in 2015 and anticipated production mix in 2050 based on NS3720 [1].

	2015		2020		CO_2 factor(g/kWh)
Production technology	NO	EU28+NO	NO	EU28+NO	
Hydro power	95%	18%	85%	8%	11 (2-20)
Wind power	1%	8%	15%	33%	22 (3-41)
Thermal power Norway	4%				450
Thermal power EU		43%			80
PV		3%		10%	100 (13-190)
Geo/biothermal		0.4%		10%	59 (8.5-130)
Nuclear		28%		19%	566 (380-1000)
Thermal power CCS				20%	100

S3.2 | PV system

The PV system is similar to the one at the ZEB Skarpnes [21], with fully building integrated PV system. The PV degradation is accounted for according to Equation S3.1. where E (kWh/year) is the first year's energy yield, i.e. the IDA ICE output, d_{int} (%) is the initial degradation, d_{lin} (%) is the linear degradation, A_{PV} (m^2) is the module area, t_{int} (years) is the time of initial degradation, and and t is the lifetime of module, here 30 years. Table S3.2 shows the specifics for the SunPower module based on the SunPower Warranty document [119], described in detail in Fthenakis et. al [109].

$$E^t = \frac{E \cdot d_{int}}{A_{PV} \cdot t} \cdot \frac{1 - d^{t-t_{int}}}{1 - d^{t-t_{lin}}} \tag{S3.1}$$

To account for the embodied emissions in the PV system, an emission intensity for PV generation is applied. The emissions per area PV module are 281 kg CO_2EQ/m^2 based on Philippine production [109], and the energy production per square meter module area is found by applying Formula S3.1 on the simulated PV generation output from IDA ICE. The resulting emission intensity of PV generation, together with the emission intensity of electricity are shown in Figure 6 in the paper. As illustrated, the emissions are assumed halved after 30 years due to efficiency/Technology

improvements, and the average emission factor for PV is 34.08 g CO_2eq/kWh.

$$f_{PV} = \frac{g\,CO_2/m^2 module}{kWh/m^2 module} = \frac{g\,CO_2}{kWh} \tag{S3.1}$$

TABLE S3.2 Warranty for SunPower PV Modules.

Module	SunPower	Comment
Product warranty	25 years	Lifetime set to 30 years based on [109]
Performance, warranty, initial degradation	At least 95% of initial power the first five years	
Performance, warranty, annual degradation	No more than 0.4% per year (at least 87% after 25 years)	Set to 0.3%

S3.3 | District heating

The emission intensity of the district heating network is calculated based on the specific emission intensities for each of the energy sources, as suggested in the ZEB Centre. Table S3.3 provides the energy produced by source and related emissions for 2019 [108]. In conversation with BKK [120], it is informed that from 31.12.2019, fossil sources have been replaced. The effect on the carbon intensity of the production mix will not be become available until the first quarter in 2021. However, in this theses it is assumed that the fossil sources have been replaced with bio oil. Figure S3.1 illustrates the BKK district heat by energy source in 2019.

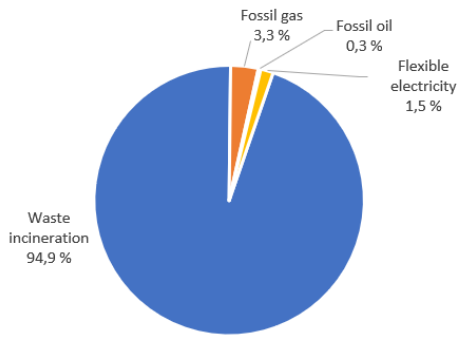

FIGURE S3.1 BKK District heat by energy source in 2019.

The emissions factors used are based on Selamwit et. al [95], and the emission factor for electricity follows the Norwegian scenario described in S3.1. It is assumed that the production mix for district heating will remain constant for the analysis period of 50 years, meaning that it will only decline due to changes in the electricity mix. Table S3.3 and S3.4 shows the associated emissions for 2019 and 2020 respectively, representing the district heating network in Bergen. The numbers are based on "Varedeklarasjon" [120], allocating the combustion emissions to the district heat

producer. The numbers in parenthesis are the numbers when the emissions from waste incineration are allocated to the waste producer and not to the district heating network, as described in [121]. The emissions from incineration reflects the emissions from technical equipment necessary to utilise the heat in the district heating system.

TABLE S3.3 Energy and associated emissions by energy source for district heat in Bergen, 2019.

	Energy produced	Energy delivered	Emission factor	Emissions
	GWh	GWh	g CO_2/kWh	g CO_2
Waste incineration	286.3	246.9	142.5 (11.1)	40797.8 (3177.9)
Fossil oil	0.9	0.9	285.0	256.5
Fossil gas	10.0	10.0	210.0	2100.0
Electricity	4.5	4.5	130	585.0
SUM	**301.7**	**262.3**		**43739.3**
SUM $(CO_2/kWh)_{delivered}$			**166.8 (23.2)**	

TABLE S3.4 Assumed energy and associated emissions by energy source for district heat in Bergen, 2020.

	Energy produced	Energy delivered	Emission factor	Emissions
	GWh	GWh	* g CO_2/kWh	g CO_2
Waste incineration	286.3	246.9	142.5 (11.1)	40797.8 (3177.9)
Bio oil	10.9	10.9	50.0	545.0
Electricity	4.5	4.5	26.4	585.0
SUM	**301.7**	**262.3**		**41461.5**
SUM $(CO_2/kWh)_{delivered}$			**158.1 (14.6)**	

*From ZEB Centre [95], except electricity following the scenarios described in S3.1

Figure S3.2 illustrate the evolution of emission intensity for when emissions from waste inceneration is allocated to the district heat producer (DH1) and to the waste producer (DH2).

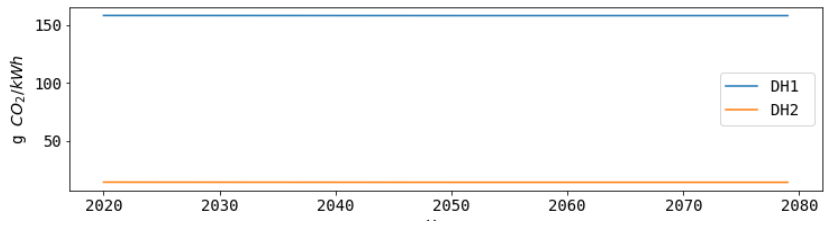

FIGURE S3.2 Evolution of emission intensity of district heating for allocating the emissions of waste incineration to the district heat producer (DH1) and to the waste producer (DH2)

S4 | CODING

The following libraries were used in the analytical tasks: 1) NumPy and SciPy for numerical computing and simulation; 2) Pandas for data wrangling; 3) Matplotlib and Seaborn for data visualisation. If codes needs to be provided, please contact the author.

Binary search pseudo code

The Load matching is based on a binary search method. Figure S4.1 exemplifies a binary search method by a flowchart representation, which is the method used to obtain the threshold value for where peak loads are shaved.

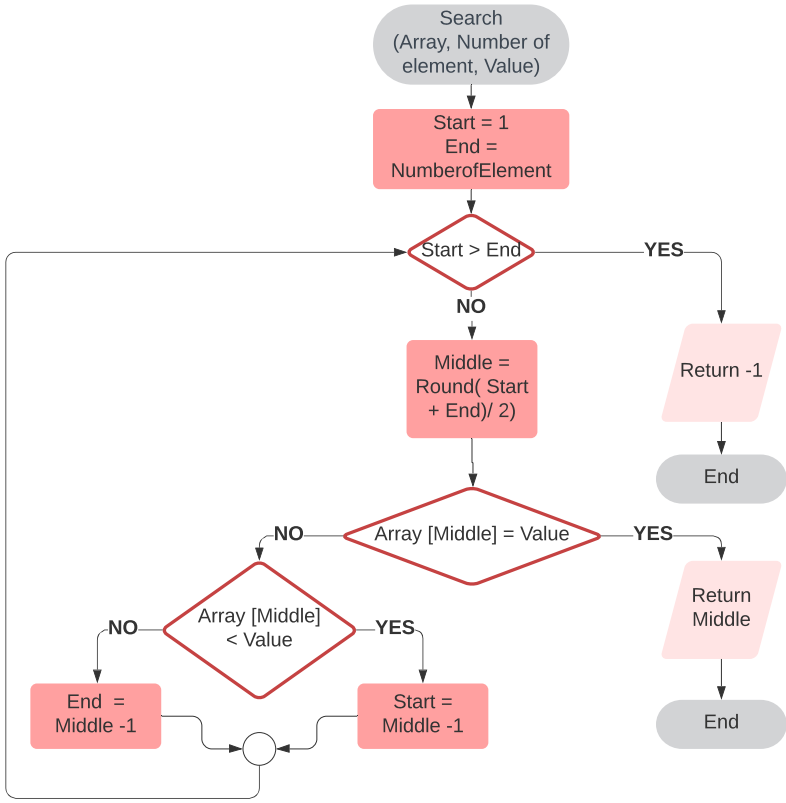

FIGURE S4.1 Flowchart of a typical binary search method, inspired by [2].

Load matching Examples

Figure S4.2 provides an example of the peak shaving strategy, where Subfigure S4.2a illustrates the binary search process, and Subfigure S4.2b illustrates the reshaped grid interaction curve. For June 1st. the neighbourhood threshold value is 2242.31 kWh, and the reshaped grid curve is negative, hence there is a net export to the grid that day.

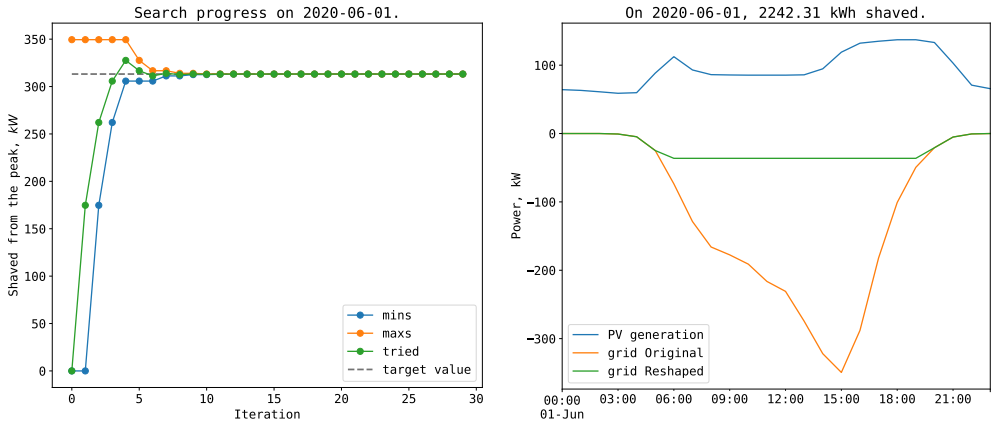

(a) Binary Search process.

(b) Reshaped curve for grid interaction.

FIGURE S4.2 Search process for battery storage with a daily peak shaving strategy on June 1st.

S5 | RESULTS

S5.1 | Load Duration Curves

Figure S5.1 and S5.2 illustrate the load duration curves for all 703 EV charging combinations for base case and the peak shaving strategies respectively.

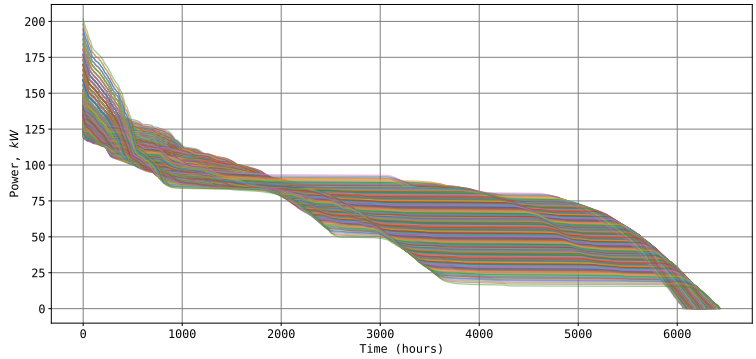

FIGURE S5.1 Load duration curves for base case, all 703 charging combinations.

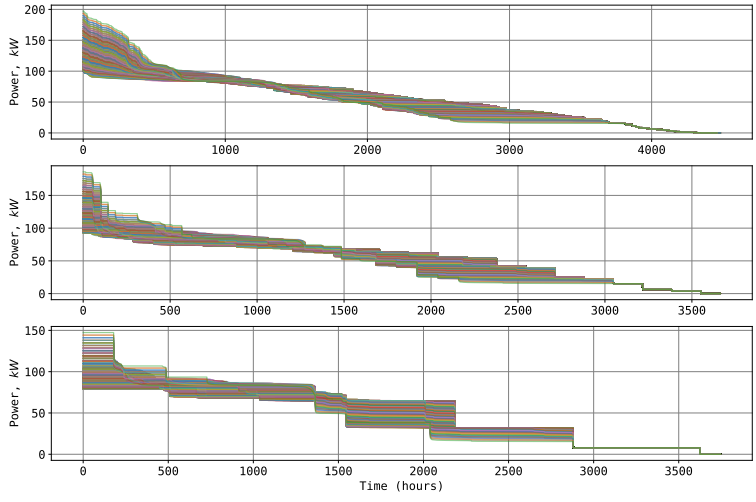

FIGURE S5.2 Load duration curves for all peak shaving strategies, all 703 charging combinations.

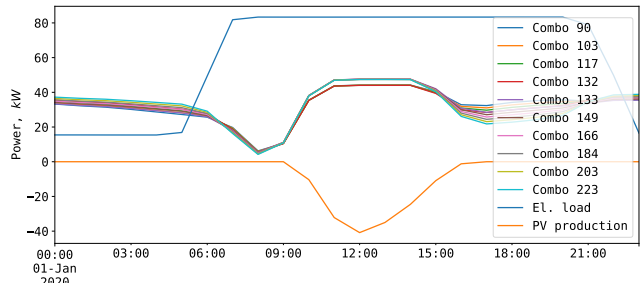

FIGURE S5.3 Top 10 charging combinations for the neighbourhoods maximum grid load performance for base case.

S5.2 | Self-consumption and Self-sufficiency

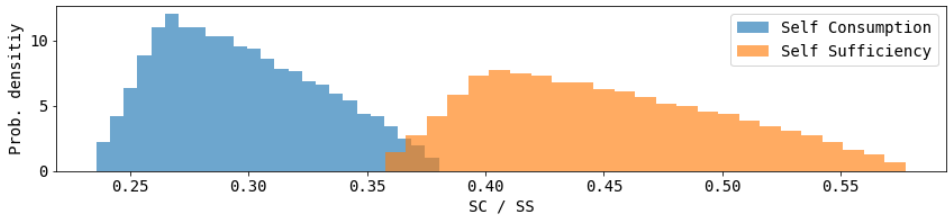

FIGURE S5.4 SC and SS for all EV combinations for base case.

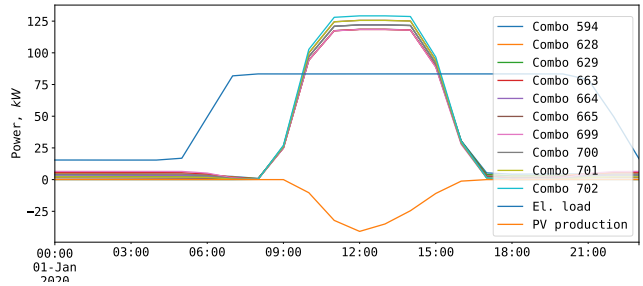

FIGURE S5.5 Top 10 charging combinations for the neighbourhoods SC and SS performance for base case.

S5.3 | Emissions

The neighbourhood emissions are distributed according to Figure Table S5.1. Here, the PV generation is first covering the building electricity demand, and then the mobility electricity demand. The higher ambition for peak shaving strat-

egy, the higher SC, thus decreased emission related to electricity import, but at the cost of total increased emissions due to storage emissions. The emissions among the different charging combinations varies more when implementing a peak shaving strategy than for base case, see Figure S5.6. Hence, the importance of charging strategy for the neighbourhood increases as peak shaving is implemented.

TABLE S5.1 Average emissions for base case and the three peak shaving strategies measured in kg CO_2eq/m^2 and year.

Scenario	$E_{B,O}$ $\frac{kgCO_2eq}{m^2yr}$	$E_{M,O}$ $\frac{kgCO_2eq}{m^2yr}$	$E_{PV,M}$ $\frac{kgCO_2eq}{m^2yr}$	$E_{DH,O}$ $\frac{kgCO_2eq}{m^2yr}$	E_{export} $\frac{kgCO_2eq}{m^2yr}$	$E_{Storage}$ $\frac{kgCO_2eq}{m^2yr}$	Total $\frac{kgCO_2eq}{m^2yr}$
Base case	0.079	0.275	2.614	0.004	-0.873	-	2.194
Daily PS	0.0	0.245	2.614	0.004	-0.669	0.528	2.722
Weekly PS	0.0	0.197	2.614	0.004	-0.621	0.664	2.858
Monthly PS	0.0	0.185	2.614	0.004	-0.609	0.705	2.899

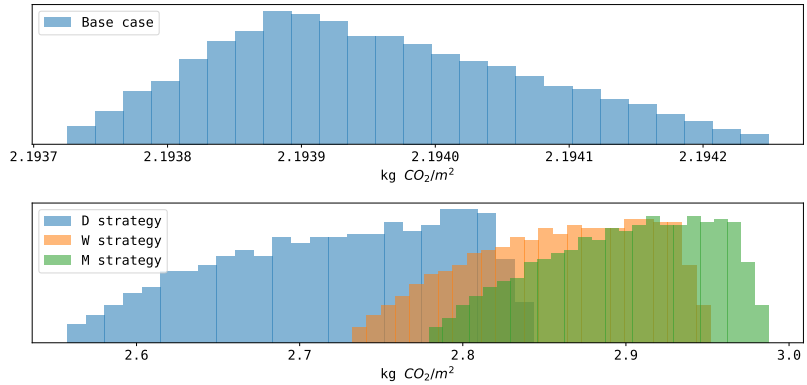

FIGURE S5.6 Distribution of emissions per square meter for Base case and for all peak shaving scenarios for all charging combination.

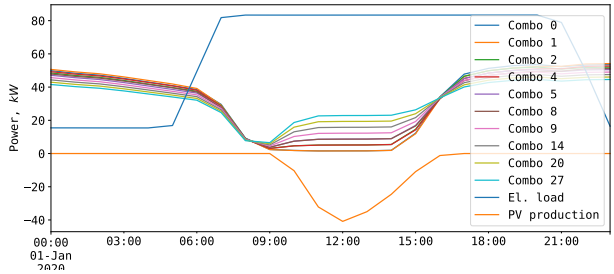

FIGURE S5.7 Top 10 charging combinations for the neighbourhoods emission performance for base case.

S5.4 | Grid-battery interaction

The following two figures illustrate the neighbourhoods energy consumption/generation and grid interaction (a) and the charge/discharge dynamics for batteries (b) for a weekly and monthly storage ambitions for charging combination one. The methodology provides this data in hourly resolution over the year for all 703 charging combinations, for all three peak shaving strategies.

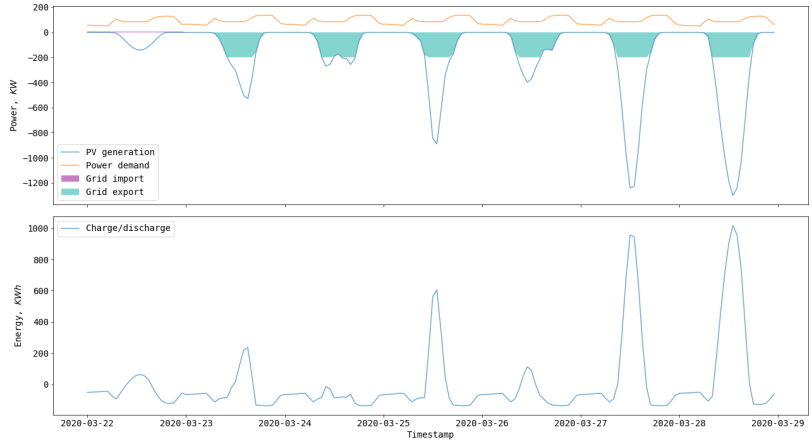

FIGURE S5.8 Charging combination one, W strategy: (a) Energy consumption and production and grid interaction: (b) Battery charge/ discharge dynamics.

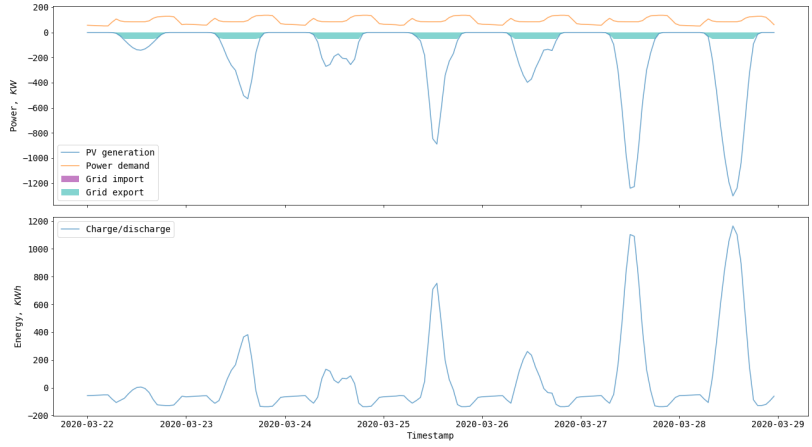

FIGURE S5.9 Charging combination one, M strategy: (a) Energy consumption and production and grid interaction: (b) Battery charge/ discharge dynamics.

S5.5 | Pair plot results

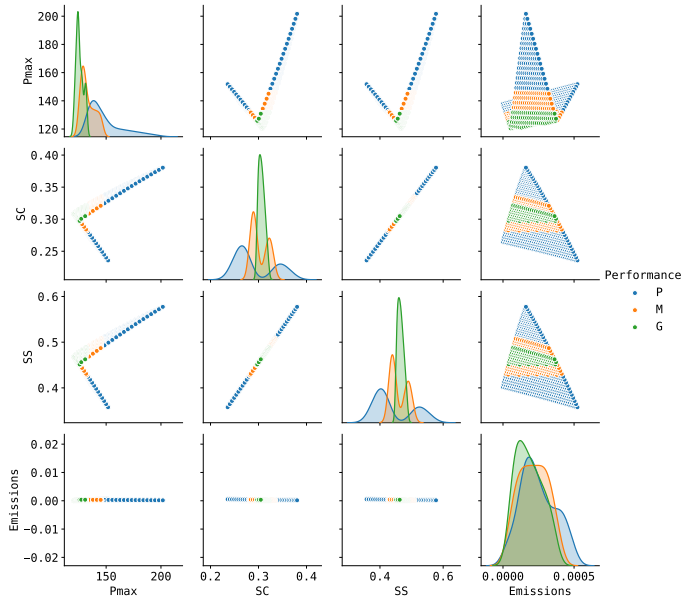

FIGURE S5.10 Pair plot of the KPIs for daily peak shaving strategy, with mean emissions restrictions.

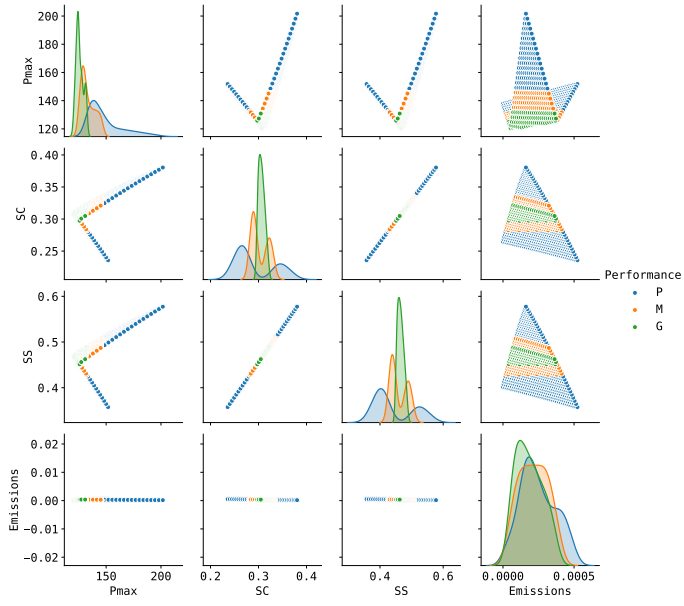

FIGURE S5.11 Pair plot of the KPIs for daily peak shaving strategy, with E_{max} restriction.

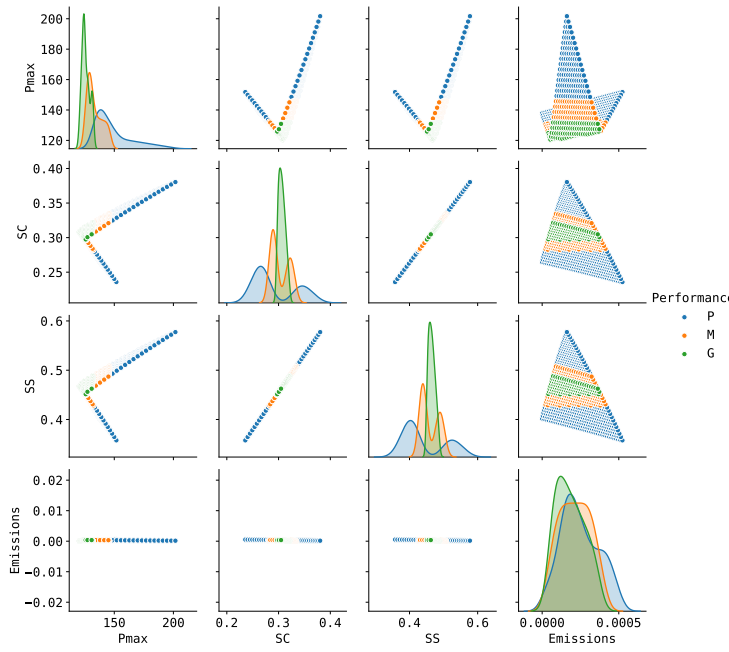

FIGURE S5.12 Pair plot of the KPIs for monthly peak shaving strategy, with mean emissions restrictions.

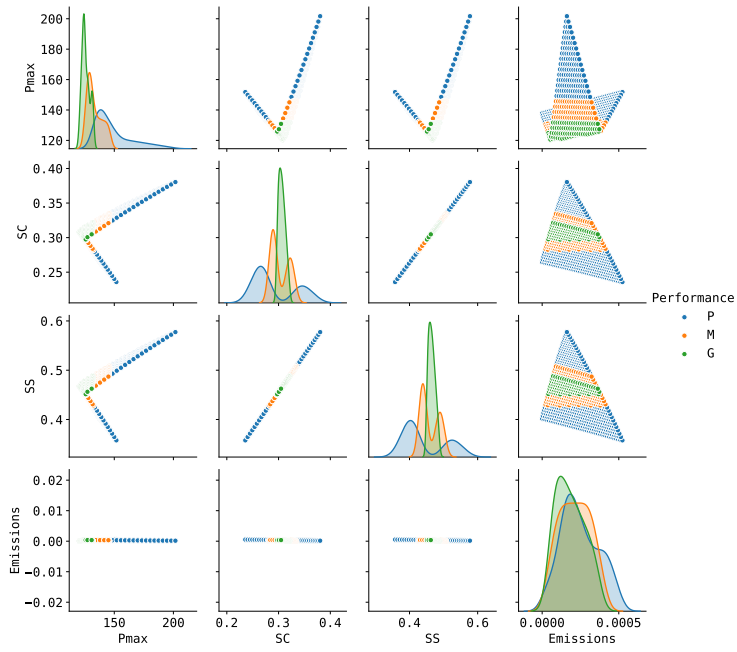

FIGURE S5.13 Pair plot of the KPIs for monthly peak shaving strategy, with E_{max} restriction.

S5.6 | Performance of charging combinations

This section contains the charging combinations satisfying the "Good", "Medium" and "Poor" performance base on criteria described in Table 5, for base case and the three peak shaving strategies with emission criteria one. The methodology makes it possible to access which charging profiles each of the charging combinations consist of, which could be useful in demand side management. The number in parenthesis is the amount of charging combinations satisfying the different performance levels.

Base case

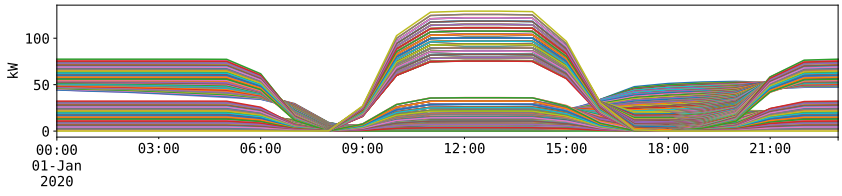

FIGURE S5.14 Charging profiles with G performance for base case (77).

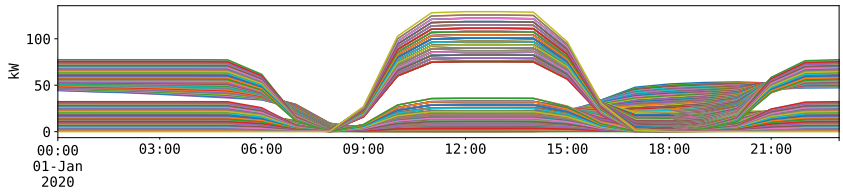

FIGURE S5.15 Charging profiles with M performance for base case (217).

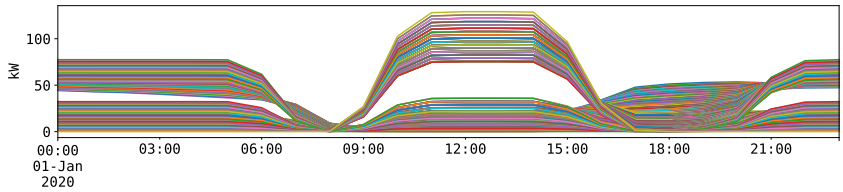

FIGURE S5.16 Charging profiles with P performance for base case (409).

Daily strategy

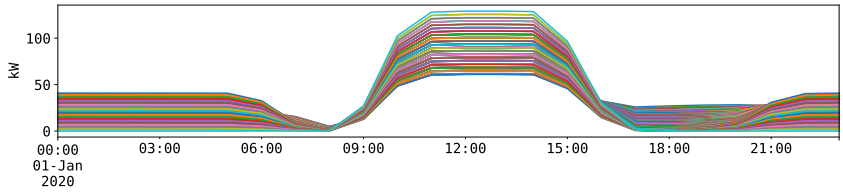

FIGURE S5.17 Charging profiles with G performance for daily strategy (8).

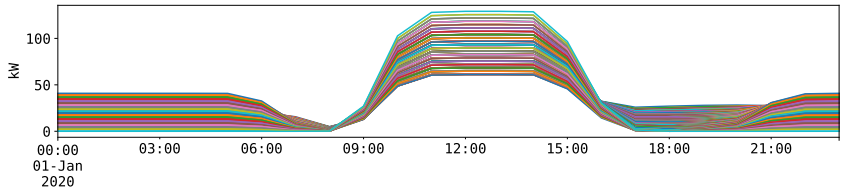

FIGURE S5.18 Charging profiles with M performance for daily strategy (485).

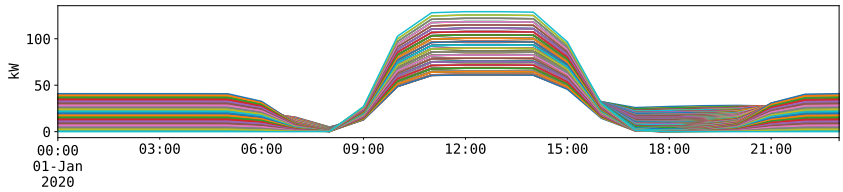

FIGURE S5.19 Charging profiles with P performance for daily strategy (210).

Weekly strategy

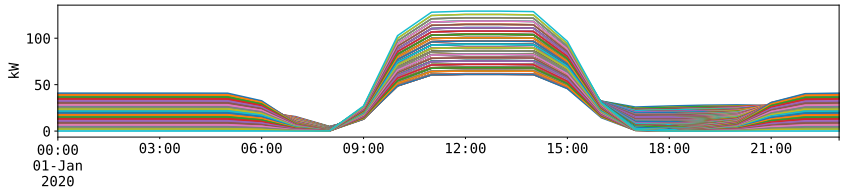

FIGURE S5.20 Charging profiles with G performance for weekly strategy (9).

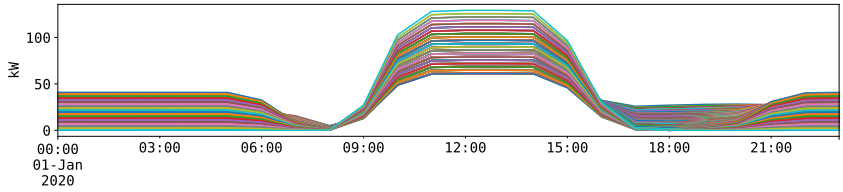

FIGURE S5.21 Charging profiles with M performance for weekly strategy (484).

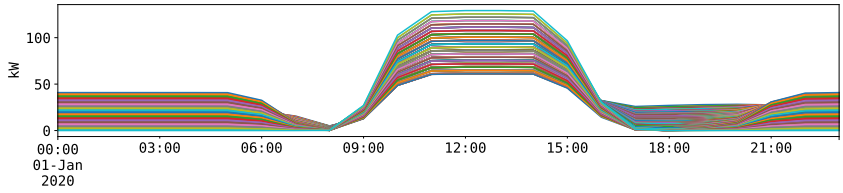

FIGURE S5.22 Charging profiles with P performance for weekly strategy (210).

Monthly strategy

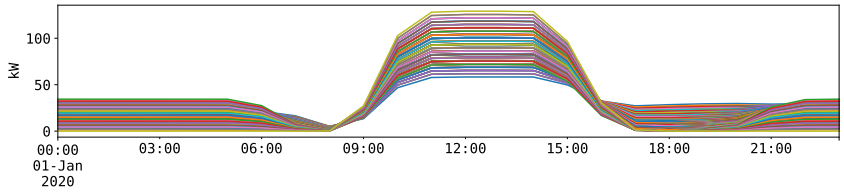

FIGURE S5.23 Charging profiles with G performance for monthly strategy (18).

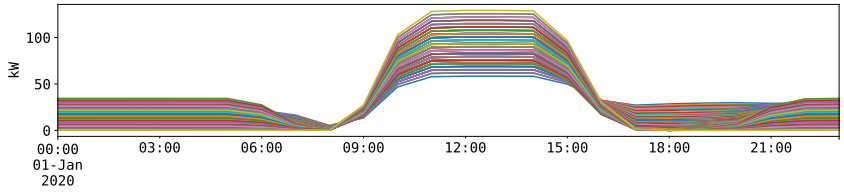

FIGURE S5.24 Charging profiles with M performance for monthly strategy (516).

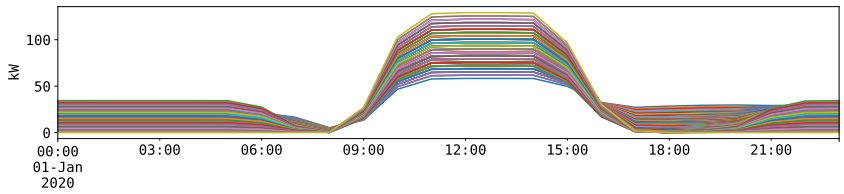

FIGURE S5.25 Charging profiles with P performance for monthly strategy (169).

S5.7 | Sensitivity analysis

S5.7.1 | Emission intensity electricity

TABLE S5.2 Average emissions for base case and the three peak shaving strategies measured in kg CO_2eq/m^2 and year

Scenario	$E_{B,O}$ $\frac{kgCO_2eq}{m^2yr}$	$E_{M,O}$ $\frac{kgCO_2eq}{m^2yr}$	$E_{PV,M}$ $\frac{kgCO_2eq}{m^2yr}$	$E_{DH,O}$ $\frac{kgCO_2eq}{m^2yr}$	E_{export} $\frac{kgCO_2eq}{m^2yr}$	$E_{Storage}$ $\frac{kgCO_2eq}{m^2yr}$	Total $\frac{kgCO_2eq}{m^2yr}$
Base case	0.079	0.275	2.614	0.004	-3.451	-	-0.384
Daily PS	0	0.245	2.614	0.004	-3.247	0.528	0.144
Weekly PS	0	0.197	2.614	0.004	-3.199	0.664	0.280
Monthly PS	0	0.185	2.614	0.004	-3.187	0.705	0.321

S5.7.2 | Emission intensity of district heat

Figure S5.3 illustrates that the total emissions are only marginally affected by a change in the emission intensity, because the neighbourhood district heat consumption is so little.

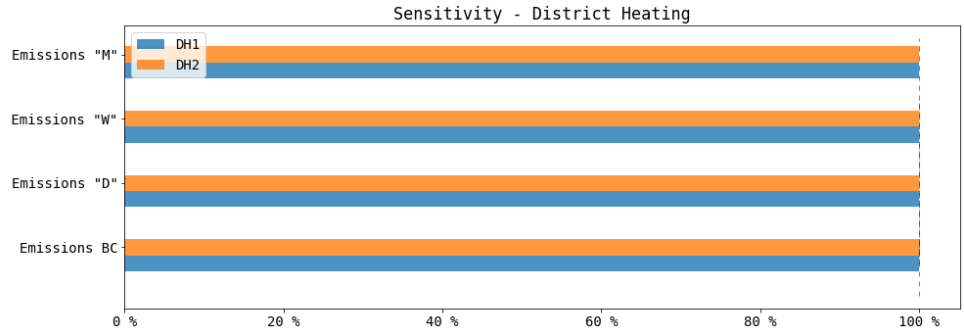

FIGURE S5.26 Relative change in total emissions when changing from DH1 to DH2.

S5.7.3 | Disregarding excess heat

Table S5.3 provides the emissions by element and life cycle stage when supply of excess heat from the power transformer is disregarded. Further, Table S5.4 provides the neighbourhood emissions if the emissions from waste incineration are allocated to the waste producer (DH2) instead of the district heat producer (DH1). Figure S5.27 illustrates that the total emissions changes significantly when there is no excess heat from the transformer.

TABLE S5.3 Average emissions for base case and the three peak shaving strategies measured in kg CO_2eq/m^2 and year when disregarding excess heat from the transformer.

Scenario	$E_{B,O}$ $\frac{kgCO_2eq}{m^2 yr}$	$E_{M,O}$ $\frac{kgCO_2eq}{m^2 yr}$	$E_{PV,M}$ $\frac{kgCO_2eq}{m^2 yr}$	$E_{DH,O}$ $\frac{kgCO_2eq}{m^2 yr}$	E_{export} $\frac{kgCO_2eq}{m^2 yr}$	$E_{Storage}$ $\frac{kgCO_2eq}{m^2 yr}$	Total $\frac{kgCO_2eq}{m^2 yr}$
Base case	0.079	0.275	2.614	4.933	-0.873	-	7.124
Daily PS	0	0.245	2.614	4.934	-0.669	0.528	7.652
Weekly PS	0	0.197	2.614	4.934	-0.621	0.664	7.788
Monthly PS	0	0.185	2.614	4.934	-0.609	0.705	7.829

TABLE S5.4 Average emissions for base case and the three peak shaving strategies measured in kg CO_2eq/m^2 and year, when disregarding excess heat from the transformer and allocating emissions from waste incineration to the waste producer.

Scenario	$E_{B,O}$ $\frac{kgCO_2eq}{m^2 yr}$	$E_{M,O}$ $\frac{kgCO_2eq}{m^2 yr}$	$E_{PV,M}$ $\frac{kgCO_2eq}{m^2 yr}$	$E_{DH,O}$ $\frac{kgCO_2eq}{m^2 yr}$	E_{export} $\frac{kgCO_2eq}{m^2 yr}$	$E_{Storage}$ $\frac{kgCO_2eq}{m^2 yr}$	Total $\frac{kgCO_2eq}{m^2 yr}$
Base case	0.079	0.275	2.614	0.455	-0.873	-	2.645
Daily PS	0	0.245	2.614	0.455	-0.669	0.528	3.173
Weekly PS	0	0.197	2.614	0.455	-0.621	0.664	3.309
Monthly PS	0	0.185	2.614	0.455	-0.609	0.705	3.350

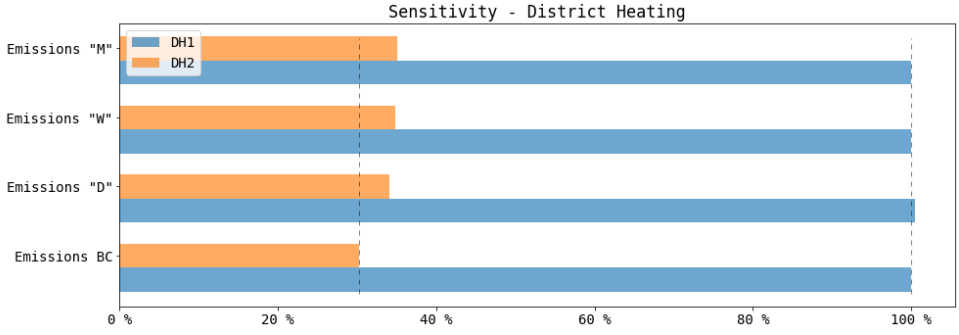

FIGURE S5.27 Relative change in total emissions when changing from DH1 to DH2, when the neighbourhood has no excess heat supply.

S5.7.4 | Charging Cycles

The sensitivity analysis on number of charging cycles shows that increasing the number with 50% yields emission reduction of approximately 10% whereas reducing the charging cycles by 50% increase the total emissions by approximately 30%. This illustrates that the emissions are more sensitive to reduced cycles compared to increased number of cycles, which is due to the shorter lifetime, the more accurate will the number of replacement be within the POA. This can be seen in Figure S5.29, illustrating the extreme case of increasing/reducing number of cycles by 75%.

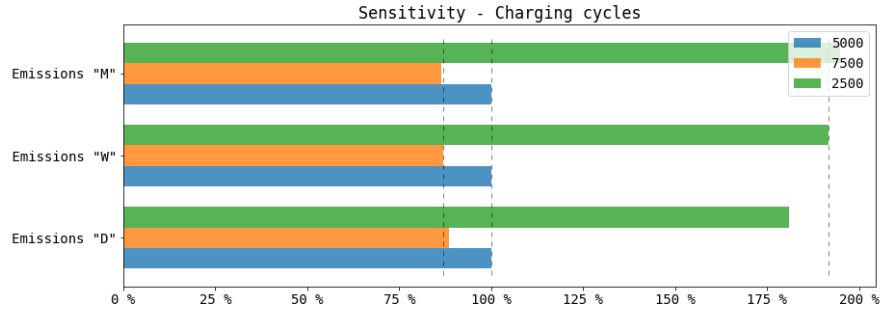

FIGURE S5.28 Sensitivity on number of Charging cycles.

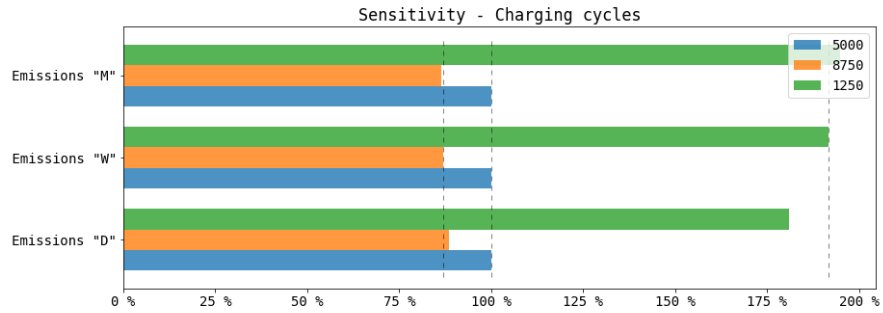

FIGURE S5.29 Sensitivity on number of Charging cycles - extreme case.

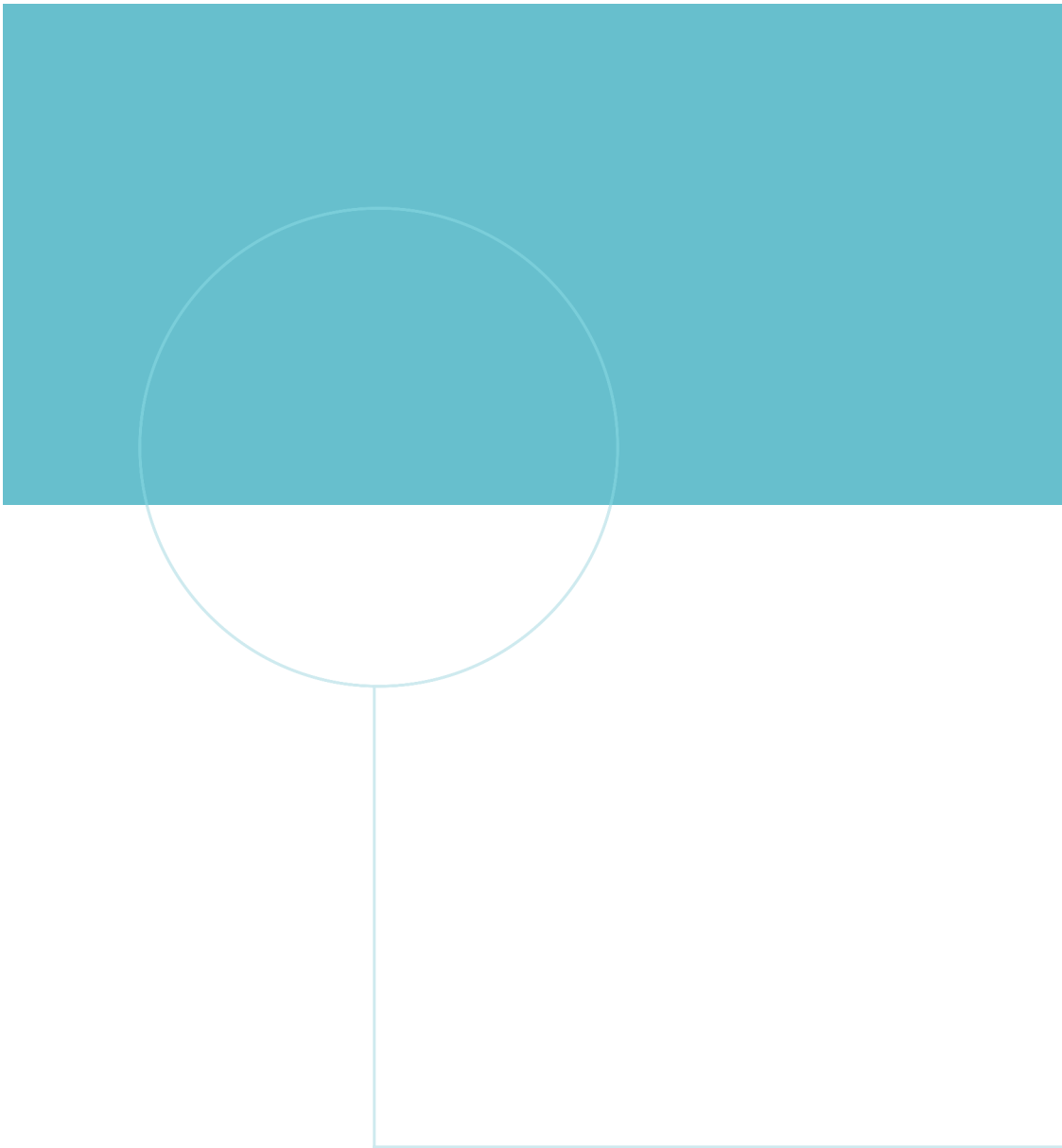

NTNU

Norwegian University of
Science and Technology